

# Quantum geometric bound for saturated ferromagnetism

Junha Kang,<sup>1,2,3</sup> Taekoo Oh,<sup>4</sup> Junhyun Lee,<sup>5</sup> and Bohm-Jung Yang<sup>1,2,3,\*</sup>

<sup>1</sup>*Department of Physics and Astronomy, Seoul National University, Seoul 08826, Korea*

<sup>2</sup>*Center for Theoretical Physics (CTP), Seoul National University, Seoul 08826, Korea*

<sup>3</sup>*Institute of Applied Physics, Seoul National University, Seoul 08826, Korea*

<sup>4</sup>*RIKEN Center for Emergent Matter Science (CEMS), Wako, Saitama 351-0198, Japan*

<sup>5</sup>*Department of Physics and Astronomy, Center for Materials Theory, Rutgers University, Piscataway, NJ 08854, United States of America*

Despite its abundance in nature, predicting the occurrence of ferromagnetism in the ground state is possible only under very limited conditions such as in a flat band system with repulsive interaction or in a band with a single hole under infinitely large Coulomb repulsion, etc. Here, we propose a general condition to achieve saturated ferromagnetism based on the quantum geometry of electronic wave functions in itinerant electron systems. By analyzing the spin excitations of multi-band repulsive Hubbard models with an integer band filling, relevant to either ferromagnetic insulators or semimetals, we show that quantum geometry stabilizes the Goldstone mode in the strongly correlated limit. Our theory indicates the stability of ferromagnetism in a large class of insulators and semimetals other than the previously studied flat band systems and their variants. Moreover, we rigorously prove that saturated ferromagnetism is forbidden in any system with trivial quantum geometry, which includes every half-filled system. We believe that our findings reveal a profound connection between quantum geometry and ferromagnetism, which can be extended to various symmetry-broken ground states in itinerant electronic systems.

*Introduction.*— Ferromagnetism is the simplest form of symmetry-broken ground states whose fundamental origin has been discussed by divergent perspectives, from Heisenberg’s localized electron picture [1] to Bloch’s itinerant electron approach [2]. More recently, the modern theory of ferromagnetism formulated based on the Hubbard model [3–5] has led to various exact theorems including the following two distinct mechanisms. One is Nagaoka’s ferromagnetism [6–8], where a single hole in the valence band induces the spin alignment when the electron repulsion is infinite. Although mathematically interesting, Nagaoka’s ferromagnetism is considered to be too fragile to exist in realistic electronic systems, as it is destroyed upon introducing a second hole [9]. The contemporary understanding is largely based on flat band ferromagnetism and its variants extensively studied by Mielke [10–13] and Tasaki [12, 14–19], where the authors construct exactly solvable models that rigorously exhibit ferromagnetism. Despite delivering valuable insights into the origin of ferromagnetism, the requirement of a flat band places a heavy constraint regarding its applicability to general systems. Thus, it is imperative to obtain a general criterion for the stability of ferromagnetism applicable to the vast majority of systems where such theorems are out of reach.

Recently, the quantum geometry of electronic wave functions has garnered increasing attention due to its relevance to various physical phenomena, such as anomalous Landau levels of flat bands [20–22], flat band superconductivity [23–25], and nonlinear Hall effect [26, 27], etc. Moreover, it has been shown that quantum geometry plays a prominent role in describing the inter-

acting ground states with spontaneous symmetry breaking [28, 29]. For instance, in superconductors, quantum geometry was shown to be deeply related to the superfluid weight [24, 30], the length scale of Cooper pairs [31, 32], and the dynamics of the Higgs mode [33]. Also, in excitonic ground states, quantum geometry was shown to induce anomalous Lamb shifts [34], contribute to the exciton drift velocity [35], and stabilize exciton condensates [36]. In contrast, the role of quantum geometry in magnetic ground states remains largely unexplored [28, 37–39].

In this Letter, we construct an exact criterion for achieving saturated ferromagnetism (SFM) in repulsive Hubbard models, applicable to any integer-filled kinetic Hamiltonian with arbitrary dimensionality and complexity, given that it becomes an insulator or semimetal upon filling one spin sector. By examining the spin excitations of the Hubbard model, we obtain an analytic expression for the Goldstone mode valid in the strongly correlated limit. We show that the stability of the Goldstone mode is governed by the quantum geometry of the non-interacting electron bands, and express the spin stiffness, which is the inverse mass of the Goldstone boson, in terms of the band-resolved quantum geometric tensors [40, 41]. This shows that the ferromagnetism of insulators or semimetals arises from the delicate interplay between Wannier function spreading and the Coulomb repulsion, similar to Heisenberg’s ferromagnetism [1]. Moreover, by identifying the aforementioned expression as a rigorous upper bound of the Goldstone mode, we show that saturated ferromagnetism is strictly prohibited when the quantum geometry is trivial, which formally rules out the possibility of saturated ferromagnetism in every half-filled Hubbard model.

*Saturated ferromagnetism.*— SFM represents the most

\* bjiang@snu.ac.kr

robust manifestation of ferromagnetic behavior, characterized by the ground state possessing maximum total spin [6–8, 10–19]. The highly restricted form of this configuration allows us to represent the ground state using only the information of the kinetic Hamiltonian, considerably simplifying the problem [42]. For its description, let us consider the following repulsive Hubbard model

$$H = \sum_{\mathbf{k}\alpha\beta\sigma} h(\mathbf{k})_{\alpha\beta} c_{\mathbf{k}\alpha\sigma}^\dagger c_{\mathbf{k}\beta\sigma} + U \sum_{\mathbf{R}\alpha} n_{\mathbf{R}\alpha\uparrow} n_{\mathbf{R}\alpha\downarrow}, \quad (1)$$

where  $h(\mathbf{k})$  and  $U > 0$  indicate the kinetic Hamiltonian and the local Hubbard repulsion, respectively.  $c_{\mathbf{k}\alpha\sigma}$  denotes the annihilation operator of an electron with momentum  $\mathbf{k}$ , orbital index  $\alpha = 1, \dots, N_{orb}$ , and spin  $\sigma = \uparrow, \downarrow$ .  $n_{\mathbf{R}\alpha\sigma} \equiv c_{\mathbf{R}\alpha\sigma}^\dagger c_{\mathbf{R}\alpha\sigma}$  is the corresponding number operator, and  $\mathbf{R} = \mathbf{R}_1, \dots, \mathbf{R}_{N_c}$  denotes the  $N_c$  unit cells. In addition, we fix the electron number to  $N_{tot} = N_c N_{occ}$ , and assume that upon filling one spin sector,  $h(\mathbf{k})$  exhibits a momentum-independent band filling  $N_{occ}$  [43].

Let us denote the local and total spin operators as  $\mathbf{S}_{\mathbf{R}\alpha} = \frac{1}{2} \sum_{\sigma_1, \sigma_2} c_{\mathbf{R}\alpha\sigma_1}^\dagger \boldsymbol{\sigma}_{\sigma_1\sigma_2} c_{\mathbf{R}\alpha\sigma_2}$  and  $\mathbf{S}_{tot} = \sum_{\mathbf{R}\alpha} \mathbf{S}_{\mathbf{R}\alpha}$ , respectively ( $\boldsymbol{\sigma}$  is the Pauli matrix, and we set  $\hbar = 1$ ). The system is said to exhibit SFM if and only if

$$(\mathbf{S}_{tot})^2 |GS\rangle = S_{max}(S_{max} + 1) |GS\rangle \quad (S_{max} \equiv \frac{N_{tot}}{2}) \quad (2)$$

for any ground state  $|GS\rangle$  [42]. Denoting the single-particle eigensystem as

$$\psi_{n\mathbf{k}\sigma}^\dagger = \sum_{\alpha} c_{\mathbf{k}\alpha\sigma}^\dagger |u_n(\mathbf{k})\rangle_{\alpha}, \quad h(\mathbf{k}) |u_n(\mathbf{k})\rangle = E_n(\mathbf{k}) |u_n(\mathbf{k})\rangle, \quad (3)$$

where  $|u_n(\mathbf{k})\rangle_{\alpha}$  is the  $\alpha$ -th component of the  $N_{orb} \times 1$  column vector  $|u_n(\mathbf{k})\rangle$ , the ground state manifold is fully determined by performing SU(2) rotations to the fully polarized state  $|\Phi\rangle = \prod_n^{N_{occ}} \prod_{\mathbf{k}} \psi_{n\mathbf{k}\uparrow}^\dagger |0\rangle$ , where  $|0\rangle$  is the vacuum state. Being a single Slater determinant, mean-field analysis on  $|\Phi\rangle$  is exact for any  $U$ , which allows us to rigorously investigate the strongly correlated regime in the following [43].

*Spin excitations.*— Let us describe the spin excitation spectrum of saturated ferromagnets, generally composed of the Stoner continuum and the low-energy magnon modes [44, 45]. We begin from the saturated ferromagnetic state  $|\Phi\rangle$  and denote an arbitrary spin excitation that lowers  $S_{tot}^z$  by 1 and carries momentum  $\mathbf{Q}$  as

$$|\mathbf{Q}\rangle = \sum_{\mathbf{k}} \sum_{\alpha} \sum_n^{N_{occ}} z_{\mathbf{k}\alpha n}(\mathbf{Q}) c_{\mathbf{k}+\mathbf{Q}\alpha\downarrow}^\dagger \psi_{n\mathbf{k}\uparrow} |\Phi\rangle, \quad (4)$$

where  $z_{\mathbf{k}\alpha n}(\mathbf{Q})$  is an arbitrary number. We define the spin excitation energy as

$$\mathcal{E}(\mathbf{Q}) = \frac{\langle \mathbf{Q} | H | \mathbf{Q} \rangle}{\langle \mathbf{Q} | \mathbf{Q} \rangle} - \langle \Phi | H | \Phi \rangle, \quad (5)$$

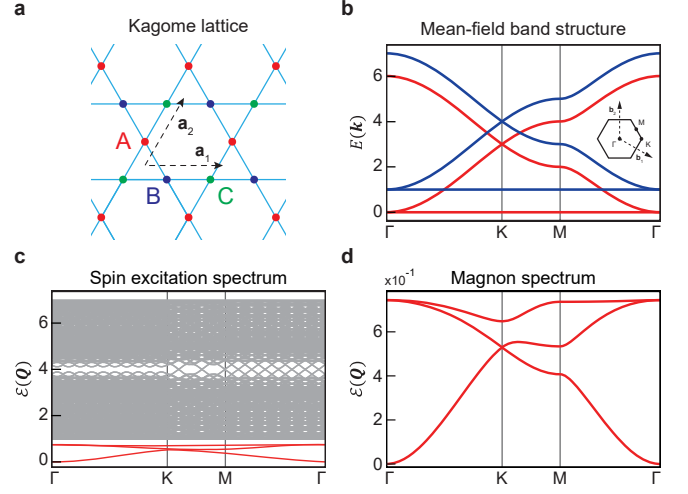


FIG. 1. **Spin excitation spectrum of the kagomé ferromagnet.** (a) The kagomé lattice. (b) The mean-field band structure for  $N_{occ} = 1$ ,  $t = 1$ ,  $U = 3$ , and  $\mu = -2$  from Eq. (8), where the lowest flat band in red is fully occupied. Red and blue lines represent the  $\uparrow$  and  $\downarrow$  spin bands, respectively. (c) The spin excitation spectrum. Red and grey lines correspond to the magnon bands and Stoner continuum, respectively. (d) The magnon band structure.

and decouple the many-body terms in Eq. (5) using mean-field theory and apply the variational principle to minimize  $\mathcal{E}(\mathbf{Q})$  with respect to  $z_{\mathbf{k}\alpha n}^*(\mathbf{Q})$  [38, 46, 47]. This gives the following eigenvalue equation

$$\sum_{\mathbf{k}'\beta n'} \mathcal{H}_{\mathbf{k}\alpha n, \mathbf{k}'\beta n'}^{SE}(\mathbf{Q}) z_{\mathbf{k}'\beta n'}(\mathbf{Q}) = \mathcal{E}(\mathbf{Q}) z_{\mathbf{k}\alpha n}(\mathbf{Q}), \quad (6)$$

where the spin excitation Hamiltonian  $\mathcal{H}^{SE}(\mathbf{Q})$  is an  $N_c N_{orb} N_{occ} \times N_c N_{orb} N_{occ}$  Hermitian matrix given by [43]

$$\begin{aligned} \mathcal{H}_{\mathbf{k}\alpha n, \mathbf{k}'\beta n'}^{SE}(\mathbf{Q}) = & [h(\mathbf{k} + \mathbf{Q})_{\alpha\beta} - E_n(\mathbf{k}) \delta_{\alpha\beta}] \delta_{\mathbf{k}\mathbf{k}'} \delta_{nn'} \\ & + \frac{U}{N_c} \left[ \sum_{\mathbf{q}} \sum_l^{N_c} \alpha \langle u_l(\mathbf{q}) | u_l(\mathbf{q}) \rangle_{\alpha} \delta_{\mathbf{k}\mathbf{k}'} \delta_{nn'} \right. \\ & \left. - \alpha \langle u_{n'}(\mathbf{k}') | u_n(\mathbf{k}) \rangle_{\alpha} \delta_{\alpha\beta} \right]. \end{aligned} \quad (7)$$

In the Supplementary Materials (SM), we prove that the mean-field decoupling in Eq. (5) is exact at any  $U > 0$  using Wick's theorem [48, 49].

For illustration, let us describe the spin excitation spectrum of a saturated ferromagnet on the kagomé lattice shown in Fig. 1 (a). The tight-binding Hamiltonian containing only the nearest-neighbor hopping amplitude  $t > 0$  is given by

$$h(\mathbf{k}) = 2t \begin{pmatrix} 0 & \cos \frac{\mathbf{k} \cdot \mathbf{a}_1}{2} & \cos \frac{\mathbf{k} \cdot \mathbf{a}_2}{2} \\ \cos \frac{\mathbf{k} \cdot \mathbf{a}_1}{2} & 0 & \cos \frac{\mathbf{k} \cdot (\mathbf{a}_1 - \mathbf{a}_2)}{2} \\ \cos \frac{\mathbf{k} \cdot \mathbf{a}_2}{2} & \cos \frac{\mathbf{k} \cdot (\mathbf{a}_1 - \mathbf{a}_2)}{2} & 0 \end{pmatrix} - \mu \mathbb{1}, \quad (8)$$

where  $\mathbf{a}_1 = (1, 0)$  and  $\mathbf{a}_2 = (\frac{1}{2}, \frac{\sqrt{3}}{2})$ ,  $\mu$  is the chemical potential, and  $\mathbb{1}$  is an identity matrix. This model has

a spin-degenerate flat band at the bottom, and exhibits SFM at any  $U > 0$  when the flat band is half filled with ( $N_{occ} = 1$ ) [10, 11, 50]. The corresponding spin-split mean-field band structure is shown in Fig. 1 (b). The relevant spin excitation spectrum in Fig. 1(c), composed of the Stoner continuum and spin wave excitations, is obtained by diagonalizing Eq. (7) at each  $\mathbf{Q}$ . In general, there are  $N_{orb}$  magnons, which consists of 1 gapless Goldstone mode and  $N_{orb} - 1$  gapped modes. When the ground state is ferromagnetic, the Goldstone mode exhibits a quadratic dispersion with an energy minimum at  $\mathbf{Q} = \mathbf{0}$ . For this reason, a positive energy in the spin excitation spectrum is regarded as a strong indicator for stable ferromagnetism [17, 44]. Conversely, a negative (or zero) magnon energy indicates that the ferromagnetic state  $|\Phi\rangle$  is unstable [9, 51].

*Approximation to the Goldstone mode.*— Assuming that  $|\Phi\rangle$  is the unique ground state up to SU(2) rotations, we use first order perturbation theory to obtain an analytic expression of the Goldstone mode. We reorganize Eq. (7) as  $\mathcal{H}^{SE}(\mathbf{Q}) = \mathcal{H}^{SE}(\mathbf{0}) + V(\mathbf{Q})$  and treat  $V(\mathbf{Q}) \equiv \mathcal{H}^{SE}(\mathbf{Q}) - \mathcal{H}^{SE}(\mathbf{0})$  as the perturbed Hamiltonian. Due to the SU(2) symmetry of  $H$ ,  $\mathcal{H}^{SE}(\mathbf{0})$  is exactly solved at  $\mathbf{Q} = \mathbf{0}$  for the Goldstone mode by  $z_{\mathbf{k}'\beta n'}(\mathbf{0}) = |u_{n'}(\mathbf{k}')\rangle_\beta$  with  $\mathcal{E}_G(\mathbf{0}) = 0$ . The Goldstone mode energy up to first order perturbation is given by  $\mathcal{E}_G^{(1)}(\mathbf{Q}) = \frac{\langle z_G^{(0)}(\mathbf{0}) | V(\mathbf{Q}) | z_G^{(0)}(\mathbf{0}) \rangle}{\langle z_G^{(0)}(\mathbf{0}) | z_G^{(0)}(\mathbf{0}) \rangle}$ , with

$$\mathcal{E}_G^{(1)}(\mathbf{Q}) = \frac{1}{N_{tot}} \sum_{\mathbf{k}} \text{Tr}[(h(\mathbf{k} + \mathbf{Q}) - h(\mathbf{k}))P(\mathbf{k})], \quad (9)$$

where  $P(\mathbf{k}) = \sum_n |u_n(\mathbf{k})\rangle\langle u_n(\mathbf{k})|$  is the occupied band projector [43]. Note that the ambiguity in choosing  $P(\mathbf{k})$  may be avoided at band crossings by shifting the momentum space grid, or using the gauge choice that returns maximally localized Wannier functions (MLWF) for entangled bands [52].

Importantly, Eq. (9) is fully determined by  $h(\mathbf{k})$ , and is independent of the interaction strength. To understand this behavior, note that perturbation theory is valid when the unperturbed Hamiltonian  $\mathcal{H}^{SE}(\mathbf{0})$  sufficiently larger than the perturbation  $V(\mathbf{Q})$ . Since all the  $U$ -dependent terms are in the former, our perturbative analysis describes  $\mathcal{E}_G(\mathbf{Q})$  in the strongly correlated limit, that is,  $U \rightarrow \infty$ . Moreover, as first order perturbation uses the ground state of the unperturbed Hamiltonian to calculate the energy of the perturbed Hamiltonian, it places a rigorous upper bound on the true ground state energy at any  $U$  [43]. Thus, we obtain the following inequality

$$\mathcal{E}_G(\mathbf{Q})|_{U < \infty} \leq \mathcal{E}_G(\mathbf{Q})|_{U \rightarrow \infty} \leq \mathcal{E}_G^{(1)}(\mathbf{Q}). \quad (10)$$

Let us comment on the validity of this approximation. The many-body spectrum, and consequently, the spin-excitation spectrum, is invariant upon shifting the orbital positions while retaining the hopping amplitudes. However, such transformation affects  $\mathcal{E}_G^{(1)}(\mathbf{Q})$  [43]. To obtain the optimal approximation, we enforce the minimal metric condition [28, 53], under which the lower

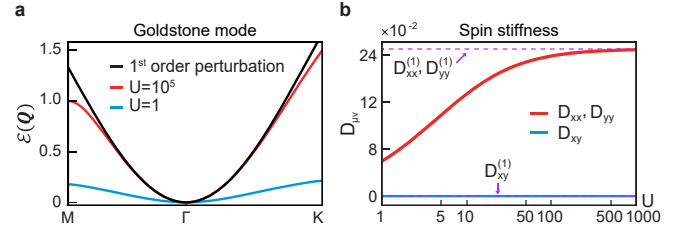


FIG. 2. **Upper bound of the Goldstone mode of the kagomé saturated ferromagnet.** (a) The Goldstone mode dispersion. Red and blue lines correspond to  $U = 10^5$  and  $U = 1$ , respectively. The black curve indicates the upper bound  $\mathcal{E}_G^{(1)}(\mathbf{Q})$ . (b) Spin stiffness  $\partial_\mu \partial_\nu \mathcal{E}_G(\mathbf{Q})|_{\mathbf{Q}=\mathbf{0}}$  as a function of  $U$ . Due to  $C_{3z}$  symmetry,  $D_{xx} = D_{yy}$  and  $D_{xy} = 0$ . The red and blue curves correspond to  $D_{xx}(D_{yy})$  and  $D_{xy}$ , respectively. The purple dashed lines obtained from  $\partial_\mu \partial_\nu \mathcal{E}_G^{(1)}(\mathbf{Q})|_{\mathbf{Q}=\mathbf{0}}$  are identical to the true spin stiffness at  $U \rightarrow \infty$ .

bound of the Wannier function spreading is minimized by varying the orbital positions. Interestingly, in all the examples we considered, the upper bound  $\mathcal{E}_G^{(1)}(\mathbf{Q})$  saturates in this position choice, as illustrated in the kagomé lattice model in Fig. 2. Even if this were not the case,  $\mathcal{E}_G^{(1)}(\mathbf{Q}) > 0$  implies  $\mathcal{E}_G(\mathbf{Q})|_{U \rightarrow \infty}$  unless the second order perturbation has a larger magnitude than the first order term. Thus,  $\mathcal{E}_G^{(1)}(\mathbf{Q})$  accurately diagnoses the stability of ferromagnetism for  $U \rightarrow \infty$  given that the perturbative framework does not break down.

*Relation to quantum geometry.*— Let us discuss the geometric aspects of Eq. (9). In general, the geometry of the quantum states, or more generally, their projectors, is characterized by the Abelian quantum geometric tensor (QGT)  $\mathfrak{G}_{\mu\nu}(\mathbf{k})$  [54], where  $\mu, \nu = x, y, \dots$  indicate orthogonal coordinates. The real and imaginary parts of the QGT are related to the quantum metric [55, 56] and Berry curvature [57] by

$$\text{Re}[\mathfrak{G}_{\mu\nu}(\mathbf{k})] = \mathfrak{g}_{\mu\nu}(\mathbf{k}), \quad \text{Im}[\mathfrak{G}_{\mu\nu}(\mathbf{k})] = -\frac{1}{2}\mathcal{F}_{\mu\nu}(\mathbf{k}). \quad (11)$$

In particular, the quantum metric defines the local geometry imposed by the Hilbert-Schmidt quantum distance

$$ds^2 = \mathfrak{g}_{\mu\nu}(\mathbf{k}) dk_\mu dk_\nu, \quad s(\mathbf{k}, \mathbf{k}')^2 = N_{occ} - \text{Tr}[P(\mathbf{k})P(\mathbf{k}')], \quad (12)$$

which is  $N_{occ}$  (0) for orthogonal (identical) projectors [43], thereby introducing a natural geometric measure for the similarity between projectors.

The geometric interpretation is as follows. In the SM, we prove that  $\mathcal{E}_G^{(1)}(\mathbf{Q}) \geq 0$ . To see this, note that  $\text{Tr}[h(\mathbf{k})P(\mathbf{k})] = \sum_n^{N_{occ}} E_n(\mathbf{k})$ . On the other hand,  $\text{Tr}[h(\mathbf{k} + \mathbf{Q})P(\mathbf{k})]$  represents the sum of the expectation values of  $h(\mathbf{k} + \mathbf{Q})$  evaluated by the occupied eigenvectors

$|u_n(\mathbf{k})\rangle$ , instead of  $|u_n(\mathbf{k} + \mathbf{Q})\rangle$ . Therefore, one obtains

$$\mathcal{E}_G^{(1)}(\mathbf{Q}) \geq \frac{1}{N_{tot}} \sum_{n\mathbf{k}} (E_n(\mathbf{k} + \mathbf{Q}) - E_n(\mathbf{k})) = 0, \quad (13)$$

where the equality saturates if and only if  $P(\mathbf{k}) = P(\mathbf{k} + \mathbf{Q})$  for every  $\mathbf{k}$  at a given  $\mathbf{Q}$ . In terms of quantum geometry, this means that  $\mathcal{E}_G^{(1)}(\mathbf{Q}) > 0$  if and only if

$$f(\mathbf{Q}) \equiv \sum_{\mathbf{k}} s(\mathbf{k}, \mathbf{k} + \mathbf{Q})^2 > 0. \quad (14)$$

Since  $f(\mathbf{0}) = 0$ , the stability condition at  $\Gamma$  requires that the quantum metric integral  $G_{\mu\nu} \equiv \frac{1}{N_c} \sum_{\mathbf{k}} g_{\mu\nu}(\mathbf{k})$  is a positive definite tensor. In turn, a large quantum metric naturally enhances the stability of the Goldstone mode.

Furthermore, we obtain the spin stiffness  $D_{\mu\nu} \equiv \partial_\mu \partial_\nu \mathcal{E}_G(\mathbf{Q})|_{\mathbf{Q}=\mathbf{0}}$ , which is the inverse mass of the Goldstone boson at  $\mathbf{Q} = \mathbf{0}$ , as [43]

$$D_{\mu\nu}^{(1)} = \frac{1}{N_{tot}} \sum_{\mathbf{k}} \left[ \sum_{n \leq N_{occ}} \partial_\mu \partial_\nu E_n(\mathbf{k}) + \sum_{m > N_{occ}} \sum_{n \leq N_{occ}} (E_m(\mathbf{k}) - E_n(\mathbf{k})) (\chi_{\mu\nu}^{mn}(\mathbf{k}) + \chi_{\nu\mu}^{mn}(\mathbf{k})) \right], \quad (15)$$

where  $\chi_{\mu\nu}^{mn}(\mathbf{k}) \equiv \langle \partial_\mu u_m(\mathbf{k}) | u_n(\mathbf{k}) \rangle \langle u_n(\mathbf{k}) | \partial_\nu u_m(\mathbf{k}) \rangle$  is the *band-resolved quantum geometric tensor* [40, 41], whose sum reduces to the QGT as  $\mathfrak{G}_{\mu\nu}(\mathbf{k}) = \sum_{m > N_{occ}} \sum_{n \leq N_{occ}} \chi_{\mu\nu}^{nm}(\mathbf{k})$ . Being the product of inter-band Berry connections,  $\chi_{\mu\nu}^{mn}(\mathbf{k})$  is closely related to quantum geometry [21]. Eq. (15) explicitly shows that  $\mathcal{E}_G^{(1)}(\mathbf{Q})$  is composed of two separate terms. One is the sum of the electronic band curvature and the other is the sum of the band-resolved QGTs between the unoccupied and occupied bands weighted by their energy difference. Note that the first term vanishes if  $E_n(\mathbf{k})$  are smooth and periodic in the Brillouin zone, which is always the case for insulators; in such cases, the geometric term fully determines the spin stiffness. Moreover, even in semimetals where the first term does not vanish, there is always a geometric contribution. This is because a kink in the band structure always induces a singularity in the wave functions, leading to a diverging  $\chi_{\mu\nu}^{mn}(\mathbf{k})$  [43, 58]. These results collectively show the prominent role of quantum geometry in stabilizing the Goldstone mode in the strongly correlated limit.

We can intuitively understand the role of quantum geometry by considering Heisenberg's direct exchange interaction between two electrons, which minimizes the Coulomb repulsion for spin triplet states for localized wave functions which have a finite overlap [1, 14, 59]. Substituting the localized wave functions with the MLWFs, one can naturally think that a larger Wannier function spreading will result in a stable ferromagnetic ground state in the strongly correlated limit. Crucially,  $G_{\mu\mu}$  is the lower bound of the spreading of the MLWF

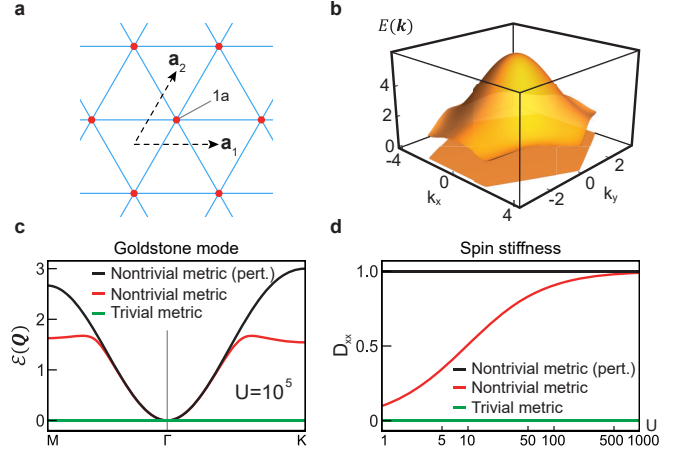


**FIG. 3. Influence of the quantum metric on the spin stiffness.** (a) Lattice structure belonging to wallpaper group  $p3$ .  $\mathbf{a}_1 = (1, 0)$  and  $\mathbf{a}_2 = (\frac{1}{2}, \frac{\sqrt{3}}{2})$  are the primitive lattice vectors. (b) The band structure of the Hamiltonian in Eq. (16). The system consists of a single occupied flat band at  $E = 0$ , which is separated from two degenerate dispersive bands. (c) Goldstone mode dispersion for  $U = 10^5$ . (d)  $D_{xx}$  plotted as a function of  $U$ . In this model,  $D_{xx} = D_{yy}$  and  $D_{xy} = 0$  due to  $C_{3z}$  symmetry. We note that  $D_{\mu\nu}(U \rightarrow \infty) = D_{\mu\nu}^{(1)}$ . In (c) and (d), the red and black curves are numerical data and the upper bound, respectively, for the model with nontrivial quantum metric. The green curves are calculated for the case with zero quantum metric.

in the  $\mu$ -th direction; conversely, the MLWFs can be perfectly localized in the  $\mu$ -th direction when  $G_{\mu\mu} = 0$  [60]. Therefore, our result shows that quantum geometry provides a natural measure of Heisenberg's direct exchange interaction, which is necessary for stabilizing SFM in integer-filled insulators or semimetals.

*No-go theorem.*— We present a no-go theorem that rigorously forbids SFM when  $G_{\mu\nu} = 0$ . Notably, this occurs for any half-filled Hubbard model, regardless of the form of  $h(\mathbf{k})$ . This is because the Wannier functions of the occupied bands can always be perfectly localized to the atomic orbitals, resulting in a vanishing direct exchange interaction. This explains the previous studies on half-filled Hubbard models, where in no circumstance has SFM been observed [61–64].

To demonstrate the influence of quantum geometry on the stability of SFM, we calculate the gapless magnon spectra of flat band models with identical energy dispersion, but different quantum metrics. Explicitly, let us consider a system in the wallpaper group  $p3$  as in Fig. 3(a), and place three orbitals whose  $C_{3z}$  eigenvalues are 1,  $\omega$ , and  $\omega^2$  ( $\omega = e^{\frac{2\pi i}{3}}$ ), respectively, at the  $1a$  Wyckoff position. Here,  $C_{3z}$  indicates a 3-fold rotation about the  $z$ -axis. We consider one occupied flat band at the Fermi level ( $E = 0$ ) and two degenerate unoccupied bands with energy  $E_{unocc}(\mathbf{k}) = 3 + \cos \mathbf{k} \cdot \mathbf{a}_1 + \cos \mathbf{k} \cdot \mathbf{a}_2 + \cos \mathbf{k} \cdot (\mathbf{a}_1 - \mathbf{a}_2)$  (Fig. 3(b)). The relevant Hamiltonian is



given by

$$h(\mathbf{k}) = E_{unocc}(\mathbf{k})(1 - P(\mathbf{k})), \quad (16)$$

where  $P(\mathbf{k}) = |u_1(\mathbf{k})\rangle\langle u_1(\mathbf{k})|$  is the occupied band projector. In these types of systems where the occupied bands are smooth and the occupied and unoccupied bands are fully degenerate among each other, the spin stiffness reduces to

$$D_{\mu\nu}^{(1)} = \frac{2}{N_{tot}} \sum_{\mathbf{k}}^{N_c} (E_m(\mathbf{k}) - E_n(\mathbf{k})) \mathbf{g}_{\mu\nu}(\mathbf{k}). \quad (17)$$

Since the quantum metric is given by  $\mathbf{g}_{\mu\nu}(\mathbf{k}) = \frac{1}{2} \text{Tr}[\partial_\mu P(\mathbf{k}) \partial_\nu P(\mathbf{k})]$ , we can tune  $\mathbf{g}_{\mu\nu}(\mathbf{k})$  by changing  $|u_1(\mathbf{k})\rangle$ . The model with zero quantum metric is constructed by using  $|u_1(\mathbf{k})\rangle = (1, 0, 0)^T$ . Following Ref. [65], we construct the geometrically nontrivial model with

$$|u_1(\mathbf{k})\rangle = \frac{1}{3} \begin{pmatrix} 1 + e^{-i\mathbf{k}\cdot\mathbf{a}_1} + e^{-i\mathbf{k}\cdot\mathbf{a}_2} \\ 1 + \omega e^{-i\mathbf{k}\cdot\mathbf{a}_1} + \omega^2 e^{-i\mathbf{k}\cdot\mathbf{a}_2} \\ 1 + \omega^2 e^{-i\mathbf{k}\cdot\mathbf{a}_1} + \omega e^{-i\mathbf{k}\cdot\mathbf{a}_2} \end{pmatrix}, \quad (18)$$

whose quantum metric is given by  $\mathbf{g}_{\mu\nu}(\mathbf{k}) = \delta_{\mu\nu}/6$ . From Eq. (17), we obtain  $D_{\mu\nu}^{(1)} = 0$  and  $\delta_{\mu\nu}$  for the trivial and nontrivial models, respectively. Fig. 3(c) and (d) show the Goldstone mode dispersion and the spin stiffness. The two models show drastically different behavior despite having the same energy dispersion, which demonstrates the significance of quantum metric on the computed quantities. Crucially, this shows that even in flat band systems which tend to exhibit SFM [10–19], the existence of a nontrivial quantum metric is required for such behavior.

*Discussion.*— We have shown that quantum geometry plays an essential role in stabilizing SFM for ferromagnetic insulators or semimetals [66–73]. This shows that even in systems completely unrelated to the extensively studied flat band models [10–19, 61], quantum geometry may provide a novel route for achieving ferromagnetism, which can potentially serve as a starting point for ferromagnetic materials search from first principles studies. We emphasize that the necessity of quantum geometry for achieving stable SFM is an exact result, valid for any Hamiltonian with integer occupation, regardless of the spatial dimension or complexity of  $h(\mathbf{k})$ . Nevertheless, one must consider the competition between different symmetry broken phases to fully characterize the ground state.

An interesting point can be made when one relates the quantum metric to various topological constraints. For instance, the well-known inequality between the trace of the quantum metric and the Berry curvature [24, 30] gives a lower bound of the quantum metric imposed by the Chern number of occupied bands, indicating that the band topology may stabilize SFM, as we demonstrate in the SM. Similarly, fragile or obstructed atomic band

topology also provides a lower bound that can be diagnosed by real space invariants developed recently [65, 74]. This shows that the existence of conducting edge states is not the only consequence of topology, in that it may influence the many-body ground state upon introducing Hubbard interaction.

Finally, we note that our theory can be directly applied to pseudospin ferromagnetism [37, 75]. Further extensions to other broken symmetry ground states in itinerant electronic systems would be one important direction for future study [29].

## ACKNOWLEDGMENTS

We thank Seung-Hun Lee and Jonah-Herzog Arbeitman for fruitful discussions regarding this work. J.K. and B.J.Y. were supported by Samsung Science and Technology Foundation under Project No. SSTF-BA2002-06, the National Research Foundation of Korea (NRF) grants funded by the government of Korea (MSIT) (Grants No. NRF-2021R1A5A1032996), and GRDC (Global Research Development Center) Cooperative Hub Program through the National Research Foundation of Korea (NRF) funded by the Ministry of Science and ICT (MSIT) (RS-2023-00258359). T.O. was supported by JSPS KAKENHI Grant Numbers 24H00197 and 24H02231.

## REFERENCES

- [1] W. Heisenberg, “Zur Theorie des Ferromagnetismus,” *Zeitschrift für Physik* **49**, 619–636 (1928).
- [2] Felix Bloch, “Bemerkung zur Elektronentheorie des Ferromagnetismus und der elektrischen Leitfähigkeit,” *Zeitschrift für Physik* **57**, 545–555 (1929).
- [3] Martin C Gutzwiller, “Effect of correlation on the ferromagnetism of transition metals,” *Physical Review Letters* **10**, 159 (1963).
- [4] Junjiro Kanamori, “Electron correlation and ferromagnetism of transition metals,” *Progress of Theoretical Physics* **30**, 275–289 (1963).
- [5] John Hubbard, “Electron correlations in narrow energy bands,” *Proceedings of the Royal Society of London. Series A. Mathematical and Physical Sciences* **276**, 238–257 (1963).
- [6] Yosuke Nagaoka, “Ferromagnetism in a narrow, almost half-filled  $s$  band,” *Physical Review* **147**, 392 (1966).
- [7] Hal Tasaki, “Extension of Nagaoka’s theorem on the large- $U$  Hubbard model,” *Physical Review B* **40**, 9192 (1989).
- [8] Hal Tasaki, “From Nagaoka’s ferromagnetism to flat-band ferromagnetism and beyond: an introduction to ferromagnetism in the Hubbard model,” *Progress of theoretical physics* **99**, 489–548 (1998).
- [9] B. S. Shastry, H. R. Krishnamurthy, and P. W. Anderson, “Instability of the Nagaoka ferromagnetic state of the  $U=\infty$  Hubbard model,” *Phys. Rev. B* **41**, 2375–2379 (1990).
- [10] Andreas Mielke, “Ferromagnetic ground states for the

- Hubbard model on line graphs,” *Journal of Physics A: Mathematical and General* **24**, L73 (1991).
- [11] A Mielke, “Exact ground states for the Hubbard model on the Kagome lattice,” *Journal of Physics A: Mathematical and General* **25**, 4335 (1992).
- [12] Andreas Mielke and Hal Tasaki, “Ferromagnetism in the Hubbard model: Examples from models with degenerate single-electron ground states,” *Communications in mathematical physics* **158**, 341–371 (1993).
- [13] Andreas Mielke, “Stability of ferromagnetism in Hubbard models with degenerate single-particle ground states,” *Journal of Physics A: Mathematical and General* **32**, 8411 (1999).
- [14] Hal Tasaki, “Ferromagnetism in the Hubbard models with degenerate single-electron ground states,” *Physical review letters* **69**, 1608 (1992).
- [15] Hal Tasaki, “Ferromagnetism in Hubbard models,” *Physical review letters* **75**, 4678 (1995).
- [16] Hal Tasaki, “Ferromagnetism in the Hubbard model: a constructive approach,” *Communications in mathematical physics* **242**, 445–472 (2003).
- [17] Hal Tasaki, “Stability of ferromagnetism in the Hubbard model,” *Physical review letters* **73**, 1158 (1994).
- [18] Hal Tasaki, “Stability of ferromagnetism in Hubbard models with nearly flat bands,” *Journal of statistical physics* **84**, 535–653 (1996).
- [19] Akinori Tanaka, “An extension of the cell-construction method for the flat-band ferromagnetism,” *Journal of Statistical Physics* **181**, 897–916 (2020).
- [20] Jun-Won Rhim, Kyoo Kim, and Bohm-Jung Yang, “Quantum distance and anomalous Landau levels of flat bands,” *Nature* **584**, 59–63 (2020).
- [21] Yoonseok Hwang, Jun-Won Rhim, and Bohm-Jung Yang, “Geometric characterization of anomalous Landau levels of isolated flat bands,” *Nature communications* **12**, 6433 (2021).
- [22] Junseo Jung, Hyeongmuk Lim, and Bohm-Jung Yang, “Quantum geometry and Landau levels of quadratic band crossings,” *Physical Review B* **109**, 035134 (2024).
- [23] Long Liang, Tuomas I Vanhala, Sebastiano Peotta, Topi Siro, Ari Harju, and Päivi Törmä, “Band geometry, Berry curvature, and superfluid weight,” *Physical Review B* **95**, 024515 (2017).
- [24] Fang Xie, Zhida Song, Biao Lian, and B Andrei Bernevig, “Topology-bounded superfluid weight in twisted bilayer graphene,” *Physical review letters* **124**, 167002 (2020).
- [25] Haidong Tian, Xueshi Gao, Yuxin Zhang, Shi Che, Tianyi Xu, Patrick Cheung, Kenji Watanabe, Takashi Taniguchi, Mohit Randeria, Fan Zhang, *et al.*, “Evidence for Dirac flat band superconductivity enabled by quantum geometry,” *Nature* **614**, 440–444 (2023).
- [26] Anyuan Gao, Yu-Fei Liu, Jian-Xiang Qiu, Barun Ghosh, Thaís V. Trevisan, Yugo Onishi, Chaowei Hu, Tiema Qian, Hung-Ju Tien, Shao-Wen Chen, *et al.*, “Quantum metric nonlinear Hall effect in a topological antiferromagnetic heterostructure,” *Science* **381**, 181–186 (2023).
- [27] Naizhou Wang, Daniel Kaplan, Zhaowei Zhang, Tobias Holder, Ning Cao, Aifeng Wang, Xiaoyuan Zhou, Feifei Zhou, Zhengzhi Jiang, Chusheng Zhang, *et al.*, “Quantum-metric-induced nonlinear transport in a topological antiferromagnet,” *Nature* **621**, 487–492 (2023).
- [28] Jonah Herzog-Arbeitman, Aaron Chew, Kukka-Emilia Huhtinen, Päivi Törmä, and B Andrei Bernevig, “Many-body superconductivity in topological flat bands,” *arXiv preprint arXiv:2209.00007* (2022), 10.48550/arXiv.2209.00007.
- [29] Zhaoyu Han, Jonah Herzog-Arbeitman, B Andrei Bernevig, and Steven A Kivelson, “Quantum Geometric Nesting” and Solvable Model Flat-Band Systems,” *Physical Review X* **14**, 041004 (2024).
- [30] Sebastiano Peotta and Päivi Törmä, “Superfluidity in topologically nontrivial flat bands,” *Nature communications* **6**, 8944 (2015).
- [31] Jin-Xin Hu, Shuai A Chen, and Kam Tuen Law, “Anomalous coherence length in superconductors with quantum metric,” *arXiv preprint arXiv:2308.05686* (2023), 10.48550/arXiv.2308.05686.
- [32] Shuai A Chen and KT Law, “Ginzburg-Landau Theory of Flat-Band Superconductors with Quantum Metric,” *Physical Review Letters* **132**, 026002 (2024).
- [33] Kristian Hauser A Villegas and Bo Yang, “Anomalous Higgs oscillations mediated by Berry curvature and quantum metric,” *Physical Review B* **104**, L180502 (2021).
- [34] Ajit Srivastava and Ataç Imamoğlu, “Signatures of Bloch-band geometry on excitons: nonhydrogenic spectra in transition-metal dichalcogenides,” *Physical review letters* **115**, 166802 (2015).
- [35] Jinlyu Cao, HA Fertig, and Luis Brey, “Quantum geometric exciton drift velocity,” *Physical Review B* **103**, 115422 (2021).
- [36] Xiang Hu, Timo Hyart, Dmitry I Pikulin, and Enrico Rossi, “Quantum-metric-enabled exciton condensate in double twisted bilayer graphene,” *Physical Review B* **105**, L140506 (2022).
- [37] B Andrei Bernevig, Biao Lian, Aditya Cowsik, Fang Xie, Nicolas Regnault, and Zhi-Da Song, “Twisted bilayer graphene. V. Exact analytic many-body excitations in Coulomb Hamiltonians: Charge gap, Goldstone modes, and absence of Cooper pairing,” *Physical Review B* **103**, 205415 (2021).
- [38] Fengcheng Wu and S Das Sarma, “Quantum geometry and stability of moiré flatband ferromagnetism,” *Physical Review B* **102**, 165118 (2020).
- [39] Päivi Törmä, “Essay: Where Can Quantum Geometry Lead Us?” *Physical Review Letters* **131**, 240001 (2023).
- [40] Hikaru Watanabe and Youichi Yanase, “Chiral photocurrent in parity-violating magnet and enhanced response in topological antiferromagnet,” *Physical Review X* **11**, 011001 (2021).
- [41] Taisei Kitamura, Akito Daido, and Youichi Yanase, “Quantum geometric effect on Fulde-Ferrell-Larkin-Ovchinnikov superconductivity,” *Physical Review B* **106**, 184507 (2022).
- [42] Hal Tasaki, *Physics and mathematics of quantum many-body systems*, Vol. 66 (Springer, 2020).
- [43] For additional information, see the Supplemental Materials.
- [44] K Kusakabe and H Aoki, “Ferromagnetic spin-wave theory in the multiband Hubbard model having a flat band,” *Physical review letters* **72**, 144 (1994).
- [45] Jenő Sólyom, *Fundamentals of the Physics of Solids: Volume 3-Normal, Broken-Symmetry, and Correlated Systems*, Vol. 3 (Springer Science & Business Media, 2010).
- [46] Ramamurti Shankar, *Principles of quantum mechanics* (Springer Science & Business Media, 2012).
- [47] David J Griffiths and Darrell F Schroeter, *Introduction to quantum mechanics* (Cambridge university press, 2018).

- [48] Gian-Carlo Wick, “The evaluation of the collision matrix,” *Physical review* **80**, 268 (1950).
- [49] Gabriele Giuliani and Giovanni Vignale, *Quantum theory of the electron liquid* (Cambridge university press, 2008).
- [50] To be precise, the kagome lattice exhibits saturated ferromagnetism when exactly half the zero-energy eigenstates including the gapless point are occupied.
- [51] Yahya Alavirad and Jay Sau, “Ferromagnetism and its stability from the one-magnon spectrum in twisted bilayer graphene,” *Physical Review B* **102**, 235123 (2020).
- [52] Ivo Souza, Nicola Marzari, and David Vanderbilt, “Maximally localized Wannier functions for entangled energy bands,” *Physical Review B* **65**, 035109 (2001).
- [53] Kukka-Emilia Huhtinen, Jonah Herzog-Arbeitman, Aaron Chew, Bogdan A Bernevig, and Päivi Törmä, “Revisiting flat band superconductivity: Dependence on minimal quantum metric and band touchings,” *Physical Review B* **106**, 014518 (2022).
- [54] Ran Cheng, “Quantum geometric tensor (fubini-study metric) in simple quantum system: A pedagogical introduction,” *arXiv preprint arXiv:1012.1337* (2010), 10.48550/arXiv.1012.1337.
- [55] JP Provost and G Vallee, “Riemannian structure on manifolds of quantum states,” *Communications in Mathematical Physics* **76**, 289–301 (1980).
- [56] Raffaele Resta, “The insulating state of matter: a geometrical theory,” *The European Physical Journal B* **79**, 121–137 (2011).
- [57] Michael Victor Berry, “Quantal phase factors accompanying adiabatic changes,” *Proceedings of the Royal Society of London. A. Mathematical and Physical Sciences* **392**, 45–57 (1984).
- [58] Yoonseok Hwang, Junseo Jung, Jun-Won Rhim, and Bohm-Jung Yang, “Wave-function geometry of band crossing points in two dimensions,” *Physical Review B* **103**, L241102 (2021).
- [59] Cécile Repellin, Zhihuan Dong, Ya-Hui Zhang, and T Senthil, “Ferromagnetism in narrow bands of moiré superlattices,” *Physical Review Letters* **124**, 187601 (2020).
- [60] Nicola Marzari and David Vanderbilt, “Maximally localized generalized Wannier functions for composite energy bands,” *Physical review B* **56**, 12847 (1997).
- [61] Elliott H Lieb, “Two theorems on the Hubbard model,” *Physical review letters* **62**, 1201 (1989).
- [62] P Fazekas, B Menge, and E Müller-Hartmann, “Ground state phase diagram of the infinite dimensional Hubbard model: A variational study,” *Zeitschrift für Physik B Condensed Matter* **78**, 69–80 (1990).
- [63] Sung-Sik Lee and Patrick A. Lee, “U(1) Gauge Theory of the Hubbard Model: Spin Liquid States and Possible Application to  $\kappa - (\text{BEDT} - \text{TTF})_2\text{Cu}_2(\text{CN})_3$ ,” *Phys. Rev. Lett.* **95**, 036403 (2005).
- [64] Aaron Szasz, Johannes Motruk, Michael P. Zaletel, and Joel E. Moore, “Chiral Spin Liquid Phase of the Triangular Lattice Hubbard Model: A Density Matrix Renormalization Group Study,” *Phys. Rev. X* **10**, 021042 (2020).
- [65] Jonah Herzog-Arbeitman, Valerio Peri, Frank Schindler, Sebastian D Huber, and B Andrei Bernevig, “Superfluid weight bounds from symmetry and quantum geometry in flat bands,” *Physical review letters* **128**, 087002 (2022).
- [66] Michael A McGuire, Hemant Dixit, Valentino R Cooper, and Brian C Sales, “Coupling of crystal structure and magnetism in the layered, ferromagnetic insulator  $\text{CrI}_3$ ,” *Chemistry of Materials* **27**, 612–620 (2015).
- [67] C Song, KW Geng, F Zeng, XB Wang, YX Shen, F Pan, YN Xie, T Liu, HT Zhou, and Z Fan, “Giant magnetic moment in an anomalous ferromagnetic insulator: Co-doped  $\text{ZnO}$ ,” *Physical Review B* **73**, 024405 (2006).
- [68] Dechao Meng, Hongli Guo, Zhangzhang Cui, Chao Ma, Jin Zhao, Jiangbo Lu, Hui Xu, Zhicheng Wang, Xiang Hu, Zhengping Fu, *et al.*, “Strain-induced high-temperature perovskite ferromagnetic insulator,” *Proceedings of the National Academy of Sciences* **115**, 2873–2877 (2018).
- [69] Xiao Zhang, Yuelei Zhao, Qi Song, Shuang Jia, Jing Shi, and Wei Han, “Magnetic anisotropy of the single-crystalline ferromagnetic insulator  $\text{Cr}_2\text{Ge}_2\text{Te}_6$ ,” *Japanese Journal of Applied Physics* **55**, 033001 (2016).
- [70] Enke Liu, Yan Sun, Nitesh Kumar, Lukas Muechler, Aili Sun, Lin Jiao, Shuo-Ying Yang, Defa Liu, Aiji Liang, Qianun Xu, *et al.*, “Giant anomalous Hall effect in a ferromagnetic kagome-lattice semimetal,” *Nature physics* **14**, 1125–1131 (2018).
- [71] Kyoo Kim, Junho Seo, Eunwoo Lee, K-T Ko, BS Kim, Bo Gyu Jang, Jong Mok Ok, Jinwon Lee, Youn Jung Jo, Woun Kang, *et al.*, “Large anomalous Hall current induced by topological nodal lines in a ferromagnetic van der Waals semimetal,” *Nature materials* **17**, 794–799 (2018).
- [72] YJ Jin, R Wang, ZJ Chen, JZ Zhao, YJ Zhao, and H Xu, “Ferromagnetic Weyl semimetal phase in a tetragonal structure,” *Physical Review B* **96**, 201102 (2017).
- [73] DF Liu, AJ Liang, EK Liu, QN Xu, YW Li, C Chen, D Pei, WJ Shi, SK Mo, P Dudin, *et al.*, “Magnetic Weyl semimetal phase in a Kagomé crystal,” *Science* **365**, 1282–1285 (2019).
- [74] Zhi-Da Song, Luis Elcoro, and B Andrei Bernevig, “Twisted bulk-boundary correspondence of fragile topology,” *Science* **367**, 794–797 (2020).
- [75] Jeil Jung, Fan Zhang, and Allan H MacDonald, “Lattice theory of pseudospin ferromagnetism in bilayer graphene: Competing interaction-induced quantum Hall states,” *Physical Review B—Condensed Matter and Materials Physics* **83**, 115408 (2011).
- [76] Per-Olov Löwdin, “On the non-orthogonality problem connected with the use of atomic wave functions in the theory of molecules and crystals,” *The Journal of Chemical Physics* **18**, 365–375 (1950).
- [77] John C Slater and George F Koster, “Simplified LCAO method for the periodic potential problem,” *Physical review* **94**, 1498 (1954).
- [78] CM Goringe, DR Bowler, and E Hernandez, “Tight-binding modelling of materials,” *Reports on Progress in Physics* **60**, 1447 (1997).
- [79] Richard Jozsa, “Fidelity for mixed quantum states,” *Journal of modern optics* **41**, 2315–2323 (1994).
- [80] Paul Güttinger, “Das verhalten von atomen im magnetischen drehfeld,” *Zeitschrift für Physik* **73**, 169–184 (1932).
- [81] Richard Phillips Feynman, “Forces in molecules,” *Physical review* **56**, 340 (1939).
- [82] Jonah-Herzog Arbeitman, private communication.
- [83] F Duncan M Haldane, “Model for a quantum Hall effect without Landau levels: Condensed-matter realization of the “parity anomaly”,” *Physical review letters* **61**, 2015 (1988).
- [84] Barry Bradlyn and Mikel Iraola, “Lecture notes on Berry phases and topology,” *SciPost Physics Lecture Notes* , 051 (2022).

# Supplemental Material for “ Quantum geometric bound for saturated ferromagnetism ”

## CONTENTS

S1. Tight-binding conventions	8
S2. Properties of the quantum geometric tensor	9
S3. The spin excitation Hamiltonian	12
S4. Spin excitations and the Goldstone mode	14
S5. Approximation to the Goldstone mode	16
S6. Numerical calculations on the no-go theorem	22
S7. Mean-field Hamiltonian of saturated ferromagnets	22

## S1. TIGHT-BINDING CONVENTIONS

In this Appendix, we introduce the tight-binding notations used throughout this letter. We consider a  $d$ -dimensional periodic lattice with  $N_c$  unit cells, spanned by the primitive lattice vectors  $\mathbf{a}_1, \dots, \mathbf{a}_d$ . The reciprocal lattice vectors are defined by  $\mathbf{a}_i \cdot \mathbf{b}_j = 2\pi\delta_{ij}$ . We denote the momentum as

$$\mathbf{k} = \sum_i k_i \mathbf{b}_i = \sum_\mu k_\mu \hat{\mathbf{e}}_\mu, \quad (\text{S1})$$

where  $i = 1, \dots, d$  and  $\mu = x, y, \dots$  index the crystalline and orthogonal coordinates, respectively. The first Brillouin zone is given by  $k_i \in [0, 1)$ .

The tight-binding Hilbert space is generated by  $c_{\mathbf{R}\alpha\sigma}^\dagger$ , which creates Löwdin orbitals at the unit cell  $\mathbf{R}$ , orbital  $\alpha = 1, \dots, N_{orb}$ , and spin  $\sigma = \uparrow, \downarrow$  [76–78]. We denote the orbital position relative to the unit cell as  $\mathbf{r}_\alpha$ . The momentum space operators are denoted as

$$c_{\mathbf{k}\alpha\sigma}^\dagger = \frac{1}{\sqrt{N_c}} \sum_{\mathbf{R}} e^{i\mathbf{k} \cdot (\mathbf{R} + \mathbf{r}_\alpha)} c_{\mathbf{R}\alpha\sigma}^\dagger, \quad c_{\mathbf{R}\alpha\sigma}^\dagger = \frac{1}{\sqrt{N_c}} \sum_{\mathbf{k}} e^{-i\mathbf{k} \cdot (\mathbf{R} + \mathbf{r}_\alpha)}. \quad (\text{S2})$$

Note that the position dependence of the orbitals has been taken account in this convention, which is crucial when dealing with quantum geometry.

We consider the standard Hubbard model with repulsive interaction  $U > 0$  [3–5]

$$\begin{aligned} H &= H_{kin} + H_{int} \\ &= \sum_{\mathbf{R}\mathbf{R}'\alpha\beta\sigma} t_{\mathbf{R},\mathbf{R}'}^{\alpha\beta} c_{\mathbf{R}\alpha\sigma}^\dagger c_{\mathbf{R}'\beta\sigma} + U \sum_{\mathbf{R}\alpha} c_{\mathbf{R}\alpha\uparrow}^\dagger c_{\mathbf{R}\alpha\downarrow}^\dagger c_{\mathbf{R}\alpha\downarrow} c_{\mathbf{R}\alpha\uparrow} \\ &= \sum_{\mathbf{k}\alpha\beta\sigma} h(\mathbf{k})_{\alpha\beta} c_{\mathbf{k}\alpha\sigma}^\dagger c_{\mathbf{k}\beta\sigma} + \frac{U}{N_c} \sum_{\mathbf{k}\mathbf{k}'\mathbf{q}\alpha} c_{\mathbf{k}+\mathbf{q}\alpha\uparrow}^\dagger c_{\mathbf{k}'-\mathbf{q}\alpha\downarrow}^\dagger c_{\mathbf{k}'\alpha\downarrow} c_{\mathbf{k}\alpha\uparrow}, \end{aligned} \quad (\text{S3})$$

where we have neglected Umklapp scattering processes in the last line. We denote the eigensystem of the single-particle Hamiltonian matrix  $h(\mathbf{k})_{\alpha\beta} = \sum_{\mathbf{R}} e^{-i\mathbf{k} \cdot (\mathbf{R} + \mathbf{r}_\alpha - \mathbf{r}_\beta)} t_{\mathbf{R}\mathbf{0}}^{\alpha\beta}$  as

$$h(\mathbf{k})|u_n(\mathbf{k})\rangle = E_n(\mathbf{k})|u_n(\mathbf{k})\rangle \quad (n = 1, \dots, N_{orb}), \quad (\text{S4})$$



where  $|u_n(\mathbf{k})\rangle$  is an  $N_{orb} \times 1$  column vector. Then, the noninteracting band electron operators are given by

$$\psi_{n\mathbf{k}\sigma}^\dagger = \sum_{\alpha} |u_n(\mathbf{k})\rangle_{\alpha} c_{\mathbf{k}\alpha\sigma}^\dagger, \quad (\text{S5})$$

where  $|u_n(\mathbf{k})\rangle_{\alpha}$  denotes the  $\alpha$ -th component of the corresponding vector.

We fix the electron number to  $N_{tot} = N_c N_{occ}$ , and assume that the saturated ferromagnetic state obtained by filling one spin sector of  $H_{kin}$  has  $N_{occ}$  occupied bands at every  $\mathbf{k}$ , which means that the system becomes a ferromagnetic insulator or semimetal. This does not mean that the noninteracting system with  $U = 0$  is insulating; in general, it is expected to be a paramagnetic metal. Throughout this Letter, we use the term ‘‘occupied bands’’ to denote the  $N_{occ}$  lowest bands of  $h(\mathbf{k})$ .

The eigenvectors of the occupied bands form an  $N_{orb} \times N_{occ}$  matrix

$$\mathcal{U}(\mathbf{k}) = (|u_1(\mathbf{k})\rangle, \dots, |u_{N_{occ}}(\mathbf{k})\rangle), \quad (\text{S6})$$

which satisfies

$$\mathcal{U}(\mathbf{k})\mathcal{U}(\mathbf{k})^\dagger = \sum_n |u_n(\mathbf{k})\rangle\langle u_n(\mathbf{k})| = P(\mathbf{k}), \quad \mathcal{U}(\mathbf{k})^\dagger\mathcal{U}(\mathbf{k}) = \mathbb{1}_{N_{occ} \times N_{occ}}, \quad (\text{S7})$$

where  $P(\mathbf{k})$  is the projector, and  $\mathbb{1}_{N_{occ} \times N_{occ}}$  is the  $N_{occ} \times N_{occ}$  identity matrix. The ambiguity in choosing  $\mathcal{U}(\mathbf{k})$  at band crossing points is avoided either by shifting the momentum space grid, or choosing the gauge which forms the maximally localized Wannier functions for entangled bands [52].

## S2. PROPERTIES OF THE QUANTUM GEOMETRIC TENSOR

In this appendix, we formulate the quantum geometric tensor (QGT) [54] using gauge-invariant projectors, and provide useful formulas for computation. Quantum geometry describes the change of occupied wave functions  $\mathcal{U}(\mathbf{k})$  in the momentum space. The central quantity is the  $d \times d$  Abelian quantum geometric tensor  $\mathfrak{G}(\mathbf{k})$ , whose entries are given by

$$\mathfrak{G}_{\mu\nu}(\mathbf{k}) = \text{Tr}[\partial_\mu \mathcal{U}(\mathbf{k})^\dagger (\mathbb{1} - P(\mathbf{k})) \partial_\nu \mathcal{U}(\mathbf{k})], \quad \partial_\mu \mathcal{U}(\mathbf{k}) \equiv \lim_{\varepsilon \rightarrow 0} \frac{\mathcal{U}(\mathbf{k} + \varepsilon \hat{\mathbf{e}}_\mu) - \mathcal{U}(\mathbf{k})}{\varepsilon}. \quad (\text{S8})$$

Note that the derivatives in this formula cannot be numerically implemented due to the gauge freedom of  $\mathcal{U}(\mathbf{k})$ . We handle this problem by obtaining an expression in terms of the gauge-invariant projectors as follows:

$$\begin{aligned} \mathfrak{G}_{\mu\nu}(\mathbf{k}) &= \text{Tr}[\partial_\mu \mathcal{U}(\mathbf{k})^\dagger (\mathbb{1} - P(\mathbf{k})) \partial_\nu \mathcal{U}(\mathbf{k}) \mathcal{U}(\mathbf{k})^\dagger \mathcal{U}(\mathbf{k})] \quad (\because \mathcal{U}(\mathbf{k})^\dagger \mathcal{U}(\mathbf{k}) = \mathbb{1}) \\ &= \text{Tr}[\mathcal{U}(\mathbf{k}) \partial_\mu \mathcal{U}(\mathbf{k})^\dagger (\mathbb{1} - P(\mathbf{k})) \partial_\nu \mathcal{U}(\mathbf{k}) \mathcal{U}(\mathbf{k})^\dagger] \quad (\because \text{Tr}[AB] = \text{Tr}[BA]) \\ &= \text{Tr}[(\partial_\mu P(\mathbf{k}) - \partial_\mu \mathcal{U}(\mathbf{k}) \mathcal{U}(\mathbf{k})^\dagger) (\mathbb{1} - P(\mathbf{k})) (\partial_\nu P(\mathbf{k}) - \mathcal{U}(\mathbf{k}) \partial_\nu \mathcal{U}(\mathbf{k})^\dagger)] \\ &= \text{Tr}[\partial_\mu P(\mathbf{k}) (\mathbb{1} - P(\mathbf{k})) \partial_\nu P(\mathbf{k})], \end{aligned} \quad (\text{S9})$$

where the last line follows from

$$P(\mathbf{k})\mathcal{U}(\mathbf{k}) = \mathcal{U}(\mathbf{k}), \quad \mathcal{U}(\mathbf{k})^\dagger P(\mathbf{k}) = \mathcal{U}(\mathbf{k})^\dagger. \quad (\text{S10})$$

We can further simplify the this expression by noting

$$P(\mathbf{k})^2 = P(\mathbf{k}) \Rightarrow \partial_\mu P(\mathbf{k}) P(\mathbf{k}) + P(\mathbf{k}) \partial_\mu P(\mathbf{k}) = \partial_\mu P(\mathbf{k}) \Rightarrow \partial_\mu P(\mathbf{k}) (\mathbb{1} - P(\mathbf{k})) = P(\mathbf{k}) \partial_\mu P(\mathbf{k}). \quad (\text{S11})$$

Therefore, we obtain the computable expression

$$\mathfrak{G}_{\mu\nu}(\mathbf{k}) = \text{Tr}[P(\mathbf{k}) \partial_\mu P(\mathbf{k}) \partial_\nu P(\mathbf{k})]. \quad (\text{S12})$$

The geometric interpretation of  $\mathfrak{G}(\mathbf{k})$  follows from its relation to the quantum metric  $\mathbf{g}(\mathbf{k})$  [55, 56] and the Berry curvature  $\mathcal{F}(\mathbf{k})$  [57]. To understand the quantum metric, let us introduce the Hilbert-Schmidt quantum distance

$$s(\mathbf{k}, \mathbf{k}')^2 = N_{occ} - \text{Tr}[P(\mathbf{k}) P(\mathbf{k}')], \quad (\text{S13})$$

which is a natural geometric measure of the dissimilarity between the occupied eigenstates  $\mathcal{U}(\mathbf{k})$  and  $\mathcal{U}(\mathbf{k}')$ .

Let us introduce some properties of the quantum distance. Firstly,  $0 \leq s(\mathbf{k}, \mathbf{k}')^2 \leq N_{occ}$ , which follows from

$$s(\mathbf{k}, \mathbf{k}')^2 = N_{occ} - \text{Tr}[\mathcal{U}(\mathbf{k})^\dagger P(\mathbf{k}') \mathcal{U}(\mathbf{k})] = N_{occ} - \sum_n \langle u_n(\mathbf{k}) | P(\mathbf{k}') | u_n(\mathbf{k}) \rangle. \quad (\text{S14})$$

Since the eigenvalues of  $P(\mathbf{k}')$  are either 0 or 1,  $0 \leq \langle u_n(\mathbf{k}) | P(\mathbf{k}') | u_n(\mathbf{k}) \rangle \leq 1$ , we obtain the desired inequality. Secondly,  $s(\mathbf{k}, \mathbf{k}')^2 = 0$  ( $N_{occ}$ ) if and only if the projectors are identical (orthogonal). To prove this statement, let us introduce two useful theorems.

*Theorem 1.*— Let us consider a Hermitian matrix  $A \succeq 0$ , where  $\succ (\succeq)$  denotes positive (semi)definiteness. Then,

$$\langle v | A | v \rangle = 0 \Leftrightarrow A | v \rangle = 0 \Leftrightarrow \langle v | A = 0 \quad (\text{S15})$$

*Proof for Theorem 1.*— Let us denote the eigensystem of  $A$  as  $A|a\rangle = a|a\rangle$ , where  $a \geq 0$ . Then, the following matrix  $B = \sum_a \sqrt{a}|a\rangle\langle a|$  is Hermitian, and satisfies  $A = B^\dagger B$ . Thus,  $\langle v | A | v \rangle = 0 \Leftrightarrow |B|v\rangle|^2 = 0 \Leftrightarrow B|v\rangle = 0 \Rightarrow A|v\rangle = 0$ . Moreover,  $A|v\rangle = 0 \Rightarrow \langle v | A | v \rangle = 0$ . Taking a Hermitian conjugate completes the proof.  $\square$

*Theorem 2.*— Let  $P = \sum_p \lambda(p)|p\rangle\langle p|$  and  $Q = \sum_q \tau(q)|q\rangle\langle q|$  denote positive semidefinite Hermitian matrices.

$$\text{Tr}[PQ] = 0 \Leftrightarrow PQ = QP = 0. \quad (\text{S16})$$

*Proof for Theorem 2.*— From Theorem 1, we find

$$\begin{aligned} \text{Tr}[PQ] &= 0 \\ &\Leftrightarrow \tau(q)\langle q | P | q \rangle = 0 \quad (\forall q) \\ &\Leftrightarrow \tau(q)P|q\rangle = 0, \quad \tau(q)\langle q | P = 0 \quad (\forall q) \\ &\Rightarrow \sum_q P\tau(q)|q\rangle\langle q| = \sum_q \tau(q)|q\rangle\langle q|P = 0 \\ &\Leftrightarrow PQ = QP = 0. \end{aligned} \quad (\text{S17})$$

Moreover,  $PQ = QP = 0 \Rightarrow \text{Tr}[PQ] = 0$  is trivial.  $\square$

Using these results, we find that the condition for maximal quantum distance is given by

$$s(\mathbf{k}, \mathbf{k}')^2 = N_{occ} \Leftrightarrow \text{Tr}[P(\mathbf{k})P(\mathbf{k}')] = 0 \Leftrightarrow P(\mathbf{k})P(\mathbf{k}') = P(\mathbf{k}')P(\mathbf{k}) = 0, \quad (\text{S18})$$

On the other hand, the condition for vanishing quantum distance is given by

$$s(\mathbf{k}, \mathbf{k}')^2 = 0 \Leftrightarrow \text{Tr}[(\mathbb{1} - P(\mathbf{k}))P(\mathbf{k}')] = 0 \Leftrightarrow P(\mathbf{k}') = P(\mathbf{k})P(\mathbf{k}') = P(\mathbf{k}')P(\mathbf{k}) \Rightarrow P(\mathbf{k}') = P(\mathbf{k}), \quad (\text{S19})$$

where we used the fact that  $\mathbb{1} - P(\mathbf{k})$  is also a projector in the first step; in the final step, we interchanged the  $\mathbf{k}$  and  $\mathbf{k}'$  indices. Since  $P(\mathbf{k}) = P(\mathbf{k}')$  trivially implies  $s(\mathbf{k}, \mathbf{k}')^2 = 0$ , we find that

$$s(\mathbf{k}, \mathbf{k}')^2 = 0 \Leftrightarrow P(\mathbf{k}) = P(\mathbf{k}'). \quad (\text{S20})$$

The quantum metric characterizes the local geometry imposed by the Hilbert-Schmidt quantum distance as  $ds^2 = \mathbf{g}_{\mu\nu}(\mathbf{k})dk_\mu dk_\nu$ . Explicitly,

$$\mathbf{g}_{\mu\nu}(\mathbf{k}) = \frac{1}{2} \frac{\partial^2 s(\mathbf{k}, \mathbf{k}')^2}{\partial k'_\mu \partial k'_\nu} \Big|_{\mathbf{k}'=\mathbf{k}} = -\frac{1}{2} \text{Tr}[P(\mathbf{k})\partial_\mu \partial_\nu P(\mathbf{k})]. \quad (\text{S21})$$

To simplify this expression, note that

$$\begin{aligned} \text{Tr}[P(\mathbf{k})^2] &= \text{Tr}[P(\mathbf{k})] = N_{occ} \\ &\Rightarrow \text{Tr}[\partial_\mu \partial_\nu P(\mathbf{k})P(\mathbf{k}) + \partial_\mu P(\mathbf{k})\partial_\nu P(\mathbf{k}) + \partial_\nu P(\mathbf{k})\partial_\mu P(\mathbf{k}) + P(\mathbf{k})\partial_\mu \partial_\nu P(\mathbf{k})] = 0 \\ &\Leftrightarrow \text{Tr}[P(\mathbf{k})\partial_\mu \partial_\nu P(\mathbf{k})] = -\text{Tr}[\partial_\mu P(\mathbf{k})\partial_\nu P(\mathbf{k})] \quad (\because \text{Tr}[AB] = \text{Tr}[BA]). \end{aligned} \quad (\text{S22})$$

Thus, the quantum metric is given by

$$\mathbf{g}_{\mu\nu}(\mathbf{k}) = \frac{1}{2} \text{Tr}[\partial_\mu P(\mathbf{k})\partial_\nu P(\mathbf{k})]. \quad (\text{S23})$$

Crucially, the quantum metric is the real part of the quantum geometric tensor. To prove this, first note that  $\mathfrak{G}(\mathbf{k}) = \mathfrak{G}(\mathbf{k})^\dagger$ , which follows from Eq. (S8):

$$\mathfrak{G}_{\mu\nu}(\mathbf{k})^* = \text{Tr}[\partial_\mu \mathcal{U}(\mathbf{k})^T (\mathbb{1} - P(\mathbf{k})^T) \partial_\nu \mathcal{U}(\mathbf{k})^*] = \text{Tr}[\partial_\nu \mathcal{U}(\mathbf{k})^\dagger (\mathbb{1} - P(\mathbf{k})) \partial_\mu \mathcal{U}(\mathbf{k})] = \mathfrak{G}_{\nu\mu}(\mathbf{k}), \quad (\text{S24})$$

where we used  $\text{Tr}[A] = \text{Tr}[A^T]$  to obtain the third equality. Thus, we obtain

$$\begin{aligned} \text{Re}[\mathfrak{G}_{\mu\nu}(\mathbf{k})] &= \frac{\mathfrak{G}_{\mu\nu}(\mathbf{k}) + \mathfrak{G}_{\nu\mu}(\mathbf{k})}{2} \quad (\because \mathfrak{G}(\mathbf{k}) = \mathfrak{G}(\mathbf{k})^\dagger) \\ &= \frac{1}{2} \text{Tr}[P(\mathbf{k})(\partial_\mu P(\mathbf{k}) \partial_\nu P(\mathbf{k}) + \partial_\nu P(\mathbf{k}) \partial_\mu P(\mathbf{k}))] \\ &= \frac{1}{2} \text{Tr}[\partial_\mu P(\mathbf{k})(\mathbb{1} - P(\mathbf{k})) \partial_\nu P(\mathbf{k}) + \partial_\mu P(\mathbf{k}) P(\mathbf{k}) \partial_\nu P(\mathbf{k})] \quad (\because \text{Tr}[AB] = \text{Tr}[BA]) \\ &= \mathfrak{g}_{\mu\nu}(\mathbf{k}). \end{aligned} \quad (\text{S25})$$

The quantum metric, in some sense, contains the information of the amplitude of the eigenvectors  $\mathcal{U}(\mathbf{k})$ . On the other hand, the Berry curvature  $\mathcal{F}(\mathbf{k})$  characterizes the geometric phase induced by the parallel transport defined by the Abelian Berry connection

$$\mathcal{A}_\mu(\mathbf{k}) = i \text{Tr}[\mathcal{U}(\mathbf{k})^\dagger \partial_\mu \mathcal{U}(\mathbf{k})]. \quad (\text{S26})$$

Explicitly,

$$\begin{aligned} \mathcal{F}_{\mu\nu}(\mathbf{k}) &= \partial_\mu \mathcal{A}_\nu(\mathbf{k}) - \partial_\nu \mathcal{A}_\mu(\mathbf{k}) \\ &= i \text{Tr}[\partial_\mu \mathcal{U}(\mathbf{k})^\dagger \partial_\nu \mathcal{U}(\mathbf{k}) + \mathcal{U}(\mathbf{k})^\dagger \partial_\mu \partial_\nu \mathcal{U}(\mathbf{k}) - \partial_\nu \mathcal{U}(\mathbf{k})^\dagger \partial_\mu \mathcal{U}(\mathbf{k}) - \mathcal{U}(\mathbf{k})^\dagger \partial_\nu \partial_\mu \mathcal{U}(\mathbf{k})] \\ &= i \text{Tr}[\partial_\mu \mathcal{U}(\mathbf{k})^\dagger \partial_\nu \mathcal{U}(\mathbf{k}) - \partial_\nu \mathcal{U}(\mathbf{k})^\dagger \partial_\mu \mathcal{U}(\mathbf{k})]. \end{aligned} \quad (\text{S27})$$

Interestingly, the imaginary part of the quantum geometric tensor is related to the Berry curvature by

$$\begin{aligned} \text{Im}[\mathfrak{G}_{\mu\nu}(\mathbf{k})] &= \frac{\mathfrak{G}_{\mu\nu}(\mathbf{k}) - \mathfrak{G}_{\nu\mu}(\mathbf{k})}{2i} \quad (\because \mathfrak{G}(\mathbf{k}) = \mathfrak{G}(\mathbf{k})^\dagger) \\ &= \frac{\text{Tr}[\partial_\mu \mathcal{U}(\mathbf{k})^\dagger (\mathbb{1} - P(\mathbf{k})) \partial_\nu \mathcal{U}(\mathbf{k}) - \partial_\nu \mathcal{U}(\mathbf{k})^\dagger (\mathbb{1} - P(\mathbf{k})) \partial_\mu \mathcal{U}(\mathbf{k})]}{2i} \\ &= -\frac{1}{2} \mathcal{F}_{\mu\nu}(\mathbf{k}) + \frac{i}{2} \text{Tr}[\partial_\mu \mathcal{U}(\mathbf{k})^\dagger \mathcal{U}(\mathbf{k}) \mathcal{U}(\mathbf{k})^\dagger \partial_\nu \mathcal{U}(\mathbf{k}) - \partial_\nu \mathcal{U}(\mathbf{k})^\dagger P(\mathbf{k}) \partial_\mu \mathcal{U}(\mathbf{k})] \\ &= -\frac{1}{2} \mathcal{F}_{\mu\nu}(\mathbf{k}) + \frac{i}{2} \text{Tr}[\mathcal{U}(\mathbf{k})^\dagger \partial_\mu \mathcal{U}(\mathbf{k}) \partial_\nu \mathcal{U}(\mathbf{k})^\dagger \mathcal{U}(\mathbf{k}) - \partial_\nu \mathcal{U}(\mathbf{k})^\dagger P(\mathbf{k}) \partial_\mu \mathcal{U}(\mathbf{k})] \\ &= -\frac{1}{2} \mathcal{F}_{\mu\nu}(\mathbf{k}) \quad (\because \text{Tr}[AB] = \text{Tr}[BA]). \end{aligned} \quad (\text{S28})$$

Note that the fourth equality follows from

$$\mathcal{U}(\mathbf{k})^\dagger \mathcal{U}(\mathbf{k}) = \mathbb{1} \Rightarrow \partial_\mu \mathcal{U}(\mathbf{k})^\dagger \mathcal{U}(\mathbf{k}) + \mathcal{U}(\mathbf{k})^\dagger \partial_\mu \mathcal{U}(\mathbf{k}) = 0 \Leftrightarrow \partial_\mu \mathcal{U}(\mathbf{k})^\dagger \mathcal{U}(\mathbf{k}) = -\mathcal{U}(\mathbf{k})^\dagger \partial_\mu \mathcal{U}(\mathbf{k}). \quad (\text{S29})$$

Thus, the following relations succinctly show the geometric aspects of  $\mathfrak{G}(\mathbf{k})$

$$\mathfrak{G}(\mathbf{k}) = \mathfrak{g}(\mathbf{k}) - \frac{i}{2} \mathcal{F}(\mathbf{k}), \quad \mathfrak{g}(\mathbf{k}) = \text{Re}[\mathfrak{G}(\mathbf{k})], \quad \mathcal{F}(\mathbf{k}) = -2 \text{Im}[\mathfrak{G}(\mathbf{k})], \quad (\text{S30})$$

which can be computed by numerically differentiating the projectors as [65]

$$\mathfrak{G}_{\mu\nu}(\mathbf{k}) = \text{Tr}[P(\mathbf{k}) \partial_\mu P(\mathbf{k}) \partial_\nu P(\mathbf{k})], \quad \mathfrak{g}_{\mu\nu}(\mathbf{k}) = \frac{1}{2} \text{Tr}[\partial_\mu P(\mathbf{k}) \partial_\nu P(\mathbf{k})], \quad \mathcal{F}_{\mu\nu}(\mathbf{k}) = i \text{Tr}[P(\mathbf{k}) [\partial_\mu P(\mathbf{k}), \partial_\nu P(\mathbf{k})]], \quad (\text{S31})$$

where the expression for the Berry curvature follows from Eq. (S12) and Eq. (S30).

### 1. Band-resolved quantum geometric tensor

Another important quantity which is closely related to quantum geometry is the *band-resolved* QGT [40, 41], also known as the *fidelity tensor* [21, 79], which characterizes the local interband transition probability through

$$p(m, \mathbf{k}; n, \mathbf{k}') = |\langle u_n(\mathbf{k}') | u_m(\mathbf{k}) \rangle|^2, \quad dp = \chi_{\mu\nu}^{mn}(\mathbf{k}) dk_\mu dk_\nu, \quad (\text{S32})$$

where  $m \neq n$ . Note that the linear term of  $dp$  vanishes, due to  $\langle u_n(\mathbf{k}) | u_m(\mathbf{k}) \rangle = 0$ . Following

$$\begin{aligned} dp &= \frac{1}{2} \frac{\partial^2 p(m, \mathbf{k}; n, \mathbf{k}')}{\partial k'_\mu \partial k'_\nu} \Big|_{\mathbf{k}'=\mathbf{k}} dk_\mu dk_\nu \\ &= \frac{1}{2} (\langle \partial_\mu u_n(\mathbf{k}) | u_m(\mathbf{k}) \rangle \langle u_m(\mathbf{k}) | \partial_\nu u_n(\mathbf{k}) \rangle + (\mu \leftrightarrow \nu)) dk_\mu dk_\nu \\ &= \langle \partial_\mu u_n(\mathbf{k}) | u_m(\mathbf{k}) \rangle \langle u_m(\mathbf{k}) | \partial_\nu u_n(\mathbf{k}) \rangle dk_\mu dk_\nu, \end{aligned} \quad (\text{S33})$$

one obtains the band-resolved QGT

$$\chi_{\mu\nu}^{mn}(\mathbf{k}) = \langle \partial_\mu u_n(\mathbf{k}) | u_m(\mathbf{k}) \rangle \langle u_m(\mathbf{k}) | \partial_\nu u_n(\mathbf{k}) \rangle, \quad (\text{S34})$$

which is a product of the non-Abelian interband Berry connections. Using the projectors of the bands  $P_n(\mathbf{k}) = |u_n(\mathbf{k})\rangle\langle u_n(\mathbf{k})|$ , one obtains the following projector formula

$$\begin{aligned} \chi_{\mu\nu}^{mn}(\mathbf{k}) &= \text{Tr} [|u_n(\mathbf{k})\rangle\langle \partial_\mu u_n(\mathbf{k}) | P_m(\mathbf{k}) | \partial_\nu u_n(\mathbf{k})\rangle\langle u_n(\mathbf{k})|] \\ &= \text{Tr} [(\partial_\mu P_n(\mathbf{k}) - |\partial_\mu u_n(\mathbf{k})\rangle\langle u_n(\mathbf{k})|) P_m(\mathbf{k}) (\partial_\nu P_n(\mathbf{k}) - |u_n(\mathbf{k})\rangle\langle \partial_\nu u_n(\mathbf{k})|)] \\ &= \text{Tr} [\partial_\mu P_n(\mathbf{k}) P_m(\mathbf{k}) \partial_\nu P_n(\mathbf{k})]. \quad (\because \langle u_n(\mathbf{k}) | P_m(\mathbf{k}) = 0, P_m(\mathbf{k}) | u_n(\mathbf{k}) \rangle = 0) \end{aligned} \quad (\text{S35})$$

Note that the name *band-resolved QGT* originates from

$$\mathfrak{G}_{\mu\nu}(\mathbf{k}) = \sum_{m > N_{occ}} \sum_{n \leq N_{occ}} \chi_{\mu\nu}^{mn}(\mathbf{k}). \quad (\text{S36})$$

### S3. THE SPIN EXCITATION HAMILTONIAN

In this Appendix, we derive the spin excitation Hamiltonian in detail. We denote the saturated ferromagnetic state as

$$|\Phi\rangle = \prod_n^{N_{occ}} \prod_{\mathbf{k}}^{N_c} \psi_{n\mathbf{k}\uparrow}^\dagger |0\rangle, \quad c_{\mathbf{k}\alpha\sigma} |0\rangle = 0, \quad (\text{S37})$$

and define spin excitations with momentum  $\mathbf{Q}$  as

$$|\mathbf{Q}\rangle = \sum_{\mathbf{k}} \sum_{\alpha}^{N_c} \sum_n^{N_{orb} N_{occ}} z_{\mathbf{k}\alpha n}(\mathbf{Q}) c_{\mathbf{k}+\mathbf{Q}\alpha\downarrow}^\dagger \psi_{n\mathbf{k}\uparrow} |\Phi\rangle = \Psi_{\mathbf{Q}}^\dagger |\Phi\rangle, \quad (\text{S38})$$

which is a weighted sum of scatterings from the  $n$ -th occupied  $\uparrow$ -spin band to all the unoccupied orbitals  $\alpha$ . The stable excitations are obtained by properly fixing  $z_{\mathbf{k}\alpha n}(\mathbf{Q})$ . Although the most physical definition is

$$[H, \Psi_{\mathbf{Q}}^\dagger] |\Phi\rangle = \mathcal{E}(\mathbf{Q}) |\mathbf{Q}\rangle, \quad (\text{S39})$$

this equation does not have an exact solution in general [45] unless the system is at half-filling. As a resolution, we define the spin excitation energy as

$$\mathcal{E}(\mathbf{Q}) = \frac{\langle \mathbf{Q} | H | \mathbf{Q} \rangle}{\langle \mathbf{Q} | \mathbf{Q} \rangle} - \langle \Phi | H | \Phi \rangle, \quad (\text{S40})$$

and perform a variation with respect to  $z_{\mathbf{k}\alpha n}^*(\mathbf{Q})$  [38, 46, 47].

To calculate the many-body correlations, we introduce Wick's theorem of normal ordering *with respect to*  $|\Phi\rangle$  [48, 49]. Let us focus on the single particle operators  $\psi_{n\mathbf{k}\uparrow}^\dagger$ , where we crucially restrict the band indices to  $n = 1, \dots, N_{occ}$ . We define the normal order with respect to  $|\Phi\rangle$  by permuting operators that annihilate  $|\Phi\rangle$  to the right with a fermionic sign. For a product of two operators, for instance, we have

$$\begin{aligned} : \psi_{n_1\mathbf{k}_1\uparrow}^\dagger \psi_{n_2\mathbf{k}_2\uparrow} : &:= -\psi_{n_2\mathbf{k}_2\uparrow}^\dagger \psi_{n_1\mathbf{k}_1\uparrow}^\dagger, & : \psi_{n_1\mathbf{k}_1\uparrow}^\dagger \psi_{n_2\mathbf{k}_2\uparrow} : &:= \psi_{n_1\mathbf{k}_1\uparrow}^\dagger \psi_{n_2\mathbf{k}_2\uparrow}^\dagger, \\ : \psi_{n_1\mathbf{k}_1\uparrow} \psi_{n_2\mathbf{k}_2\uparrow} : &:= \psi_{n_1\mathbf{k}_1\uparrow} \psi_{n_2\mathbf{k}_2\uparrow}, & : \psi_{n_1\mathbf{k}_1\uparrow}^\dagger \psi_{n_2\mathbf{k}_2\uparrow}^\dagger : &:= \psi_{n_1\mathbf{k}_1\uparrow}^\dagger \psi_{n_2\mathbf{k}_2\uparrow}^\dagger. \end{aligned} \quad (\text{S41})$$



Importantly, the expectation value of normal ordered operators on  $|\Phi\rangle$  vanish. Let us define the contraction between two operators as

$$C(AB) = AB - :AB := \langle AB \rangle, \quad (\text{S42})$$

where  $A$  and  $B$  are either  $\psi_{n\mathbf{k}\uparrow}$  or  $\psi_{n\mathbf{k}\uparrow}^\dagger$ , and  $\langle AB \rangle = \langle \Phi | AB | \Phi \rangle$ . Thus, the contraction is either 0 or 1. Wick's theorem of normal ordering is the following operator identity

$$A_1 A_2 \dots A_N = :A_1 A_2 \dots A_N : + \text{all possible contractions}, \quad (\text{S43})$$

that is, all the terms containing 1, 2, ... contractions. Note that one must perform a signful permutation to bring two operators next to each other before performing the contraction.

Let us not compute Eq. (S40). We begin with

$$\begin{aligned} I &= \langle \mathbf{Q} | H | \mathbf{Q} \rangle \\ &= \langle \mathbf{Q} | H_\uparrow + H_\downarrow + H_{int} | \mathbf{Q} \rangle \\ &= I_\uparrow + I_\downarrow + I_{int}. \end{aligned} \quad (\text{S44})$$

For later convenience, we express the Hamiltonians above as

$$\begin{aligned} H_\sigma &= \sum_{\mathbf{k}\alpha\beta} h(\mathbf{k})_{\alpha\beta} c_{\mathbf{k}\alpha\sigma}^\dagger c_{\mathbf{k}\beta\sigma} = \sum_{n\mathbf{k}} E_n(\mathbf{k}) \psi_{n\mathbf{k}\sigma}^\dagger \psi_{n\mathbf{k}\sigma}, \\ H_{int} &= \frac{U}{N_c} \sum_{\mathbf{k}\mathbf{k}'\mathbf{q}\alpha} c_{\mathbf{k}+\mathbf{q}\alpha\uparrow}^\dagger c_{\mathbf{k}'-\mathbf{q}\alpha\downarrow}^\dagger c_{\mathbf{k}'\alpha\downarrow} c_{\mathbf{k}\alpha\uparrow} = \frac{U}{N_c} \sum_{\mathbf{k}\mathbf{k}'\mathbf{q}\alpha} \sum_{l_1 l_2} \alpha \langle u_{l_1}(\mathbf{k} + \mathbf{q}) | u_{l_2}(\mathbf{k}) \rangle_\alpha \psi_{l_1 \mathbf{k} + \mathbf{q}\uparrow}^\dagger c_{\mathbf{k}'-\mathbf{q}\alpha\downarrow}^\dagger c_{\mathbf{k}'\alpha\downarrow} \psi_{l_2 \mathbf{k}\uparrow}. \end{aligned} \quad (\text{S45})$$

Proceeding with  $I_\uparrow$ , we obtain

$$\begin{aligned} I_\uparrow &= \sum_{\mathbf{k}_1 \alpha_1 n_1} \sum_{\mathbf{k}_2 \alpha_2 n_2} z_{\mathbf{k}_1 \alpha_1 n_1}^*(\mathbf{Q}) z_{\mathbf{k}_2 \alpha_2 n_2}(\mathbf{Q}) \sum_{n\mathbf{k}} E_n(\mathbf{k}) \langle \psi_{n_1 \mathbf{k}_1 \uparrow}^\dagger c_{\mathbf{k}_1 + \mathbf{Q} \alpha_1 \downarrow} \psi_{n\mathbf{k}\uparrow}^\dagger \psi_{n\mathbf{k}\uparrow} c_{\mathbf{k}_2 + \mathbf{Q} \alpha_2 \downarrow}^\dagger \psi_{n_2 \mathbf{k}_2 \uparrow} \rangle \\ &= \sum_{\mathbf{k}_1 \alpha_1 n_1 n_2} z_{\mathbf{k}_1 \alpha_1 n_1}^*(\mathbf{Q}) z_{\mathbf{k}_1 \alpha_1 n_2}(\mathbf{Q}) \sum_{n\mathbf{k}} E_n(\mathbf{k}) \langle \psi_{n_1 \mathbf{k}_1 \uparrow}^\dagger \psi_{n\mathbf{k}\uparrow}^\dagger \psi_{n\mathbf{k}\uparrow} \psi_{n_2 \mathbf{k}_1 \uparrow} \rangle. \end{aligned} \quad (\text{S46})$$

Considering only finite contributions, we can restrict the band index as  $n = 1, \dots, N_{occ}$ , which allows us to use Wick's theorem. Thus, we find

$$I_\uparrow = \sum_{\mathbf{k}\alpha n} |z_{\mathbf{k}\alpha n}(\mathbf{Q})|^2 \sum_{l\mathbf{q}} E_l(\mathbf{q}) - \sum_{\mathbf{k}\alpha n} |z_{\mathbf{k}\alpha n}(\mathbf{Q})|^2 E_n(\mathbf{k}). \quad (\text{S47})$$

Calculating the second term, we obtain

$$\begin{aligned} I_\downarrow &= \sum_{\mathbf{k}_1 \alpha_1 n_1} \sum_{\mathbf{k}_2 \alpha_2 n_2} z_{\mathbf{k}_1 \alpha_1 n_1}^*(\mathbf{Q}) z_{\mathbf{k}_2 \alpha_2 n_2}(\mathbf{Q}) \sum_{\mathbf{k}\alpha\beta} h(\mathbf{k})_{\alpha\beta} \langle \psi_{n_1 \mathbf{k}_1 \uparrow}^\dagger c_{\mathbf{k}_1 + \mathbf{Q} \alpha_1 \downarrow} c_{\mathbf{k}\alpha\downarrow}^\dagger c_{\mathbf{k}\beta\downarrow} c_{\mathbf{k}_2 + \mathbf{Q} \alpha_2 \downarrow}^\dagger \psi_{n_2 \mathbf{k}_2 \uparrow} \rangle \\ &= \sum_{\mathbf{k}_1 n_1 \alpha_1} \sum_{\mathbf{k}_2 n_2 \alpha_2} z_{\mathbf{k}_1 \alpha_1 n_1}^*(\mathbf{Q}) z_{\mathbf{k}_2 \alpha_2 n_2}(\mathbf{Q}) \sum_{\alpha} h(\mathbf{k}_2 + \mathbf{Q})_{\alpha\alpha_2} \langle \psi_{n_1 \mathbf{k}_1 \uparrow}^\dagger c_{\mathbf{k}_1 + \mathbf{Q} \alpha_1 \downarrow} c_{\mathbf{k}_2 + \mathbf{Q} \alpha \downarrow}^\dagger \psi_{n_2 \mathbf{k}_2 \uparrow} \rangle \\ &= \sum_{\mathbf{k}\alpha\beta n} z_{\mathbf{k}\alpha n}^*(\mathbf{Q}) z_{\mathbf{k}\beta n}(\mathbf{Q}) h(\mathbf{k} + \mathbf{Q})_{\alpha\beta}. \end{aligned} \quad (\text{S48})$$

The third term,  $I_{int}$ , is expressed as

$$\begin{aligned} I_{int} &= \frac{U}{N_c} \sum_{\mathbf{k}_1 \alpha_1 n_1} \sum_{\mathbf{k}_2 \alpha_2 n_2} z_{\mathbf{k}_1 \alpha_1 n_1}^*(\mathbf{Q}) z_{\mathbf{k}_2 \alpha_2 n_2}(\mathbf{Q}) \sum_{\mathbf{k}\mathbf{k}'\mathbf{q}\alpha} \sum_{l_1 l_2} \alpha \langle u_{l_1}(\mathbf{k} + \mathbf{q}) | u_{l_2}(\mathbf{k}) \rangle_\alpha \\ &\quad \times \langle \psi_{n_1 \mathbf{k}_1 \uparrow}^\dagger c_{\mathbf{k}_1 + \mathbf{Q} \alpha_1 \downarrow} \psi_{l_1 \mathbf{k} + \mathbf{q}\uparrow}^\dagger c_{\mathbf{k}'-\mathbf{q}\alpha\downarrow}^\dagger c_{\mathbf{k}'\alpha\downarrow} \psi_{l_2 \mathbf{k}\uparrow} c_{\mathbf{k}_2 + \mathbf{Q} \alpha_2 \downarrow}^\dagger \psi_{n_2 \mathbf{k}_2 \uparrow} \rangle \\ &= -\frac{U}{N_c} \sum_{\mathbf{k}_1 \alpha_1 n_1} \sum_{\mathbf{k}_2 \alpha_2 n_2} z_{\mathbf{k}_1 \alpha_1 n_1}^*(\mathbf{Q}) z_{\mathbf{k}_2 \alpha_2 n_2}(\mathbf{Q}) \sum_{\mathbf{k}\mathbf{q} l_1 l_2} \alpha_2 \langle u_{l_1}(\mathbf{k} + \mathbf{q}) | u_{l_2}(\mathbf{k}) \rangle_{\alpha_2} \\ &\quad \times \langle \psi_{n_1 \mathbf{k}_1 \uparrow}^\dagger c_{\mathbf{k}_1 + \mathbf{Q} \alpha_1 \downarrow} \psi_{l_1 \mathbf{k} + \mathbf{q}\uparrow}^\dagger c_{\mathbf{k}_2 + \mathbf{Q} - \mathbf{q} \alpha_2 \downarrow}^\dagger \psi_{l_2 \mathbf{k}\uparrow} \psi_{n_2 \mathbf{k}_2 \uparrow} \rangle \end{aligned}$$

$$= \frac{U}{N_c} \sum_{\mathbf{k}_1 \mathbf{k}_2 \alpha_1 n_1 n_2} z_{\mathbf{k}_1 \alpha_1 n_1}^*(\mathbf{Q}) z_{\mathbf{k}_2 \alpha_1 n_2}(\mathbf{Q}) \sum_{\mathbf{k} l_1 l_2} \alpha_1 \langle u_{l_1}(\mathbf{k} + \mathbf{k}_2 - \mathbf{k}_1) | u_{l_2}(\mathbf{k}) \rangle_{\alpha_1} \langle \psi_{n_1 \mathbf{k}_1 \uparrow}^\dagger \psi_{l_1 \mathbf{k} + \mathbf{k}_2 - \mathbf{k}_1 \uparrow}^\dagger \psi_{l_2 \mathbf{k} \uparrow} \psi_{n_2 \mathbf{k}_2 \uparrow} \rangle. \quad (\text{S49})$$

Again, we may restrict the  $l_1, l_2$  indices to  $1, \dots, N_{occ}$ . Applying Wick's theorem, we obtain

$$I_{int} = \frac{U}{N_c} \sum_{\mathbf{k} \alpha n} \left( |z_{\mathbf{k} \alpha n}(\mathbf{Q})|^2 \sum_{\mathbf{q} l} \alpha \langle u_l(\mathbf{q}) | u_l(\mathbf{q}) \rangle_{\alpha} - \sum_{\mathbf{k}' n'} z_{\mathbf{k} \alpha n}^*(\mathbf{Q}) z_{\mathbf{k}' \alpha n'}(\mathbf{Q})_{\alpha} \langle u_{n'}(\mathbf{k}') | u_n(\mathbf{k}) \rangle_{\alpha} \right). \quad (\text{S50})$$

The two remaining terms are given by

$$\begin{aligned} \langle H \rangle &= \sum_n \sum_{\mathbf{k}} E_n(\mathbf{k}), \\ \langle \mathbf{Q} | \mathbf{Q} \rangle &= \sum_{\mathbf{k}_1 \alpha_1 n_1} \sum_{\mathbf{k}_2 \alpha_2 n_2} z_{\mathbf{k}_1 \alpha_1 n_1}^*(\mathbf{Q}) z_{\mathbf{k}_2 \alpha_2 n_2}(\mathbf{Q}) \langle \psi_{n_1 \mathbf{k}_1 \uparrow}^\dagger c_{\mathbf{k}_1 + \mathbf{Q} \alpha_1 \downarrow}^\dagger c_{\mathbf{k}_2 + \mathbf{Q} \alpha_2 \downarrow}^\dagger \psi_{n_2 \mathbf{k}_2 \uparrow} \rangle = \sum_{\mathbf{k} \alpha n} |z_{\mathbf{k} \alpha n}(\mathbf{Q})|^2. \end{aligned} \quad (\text{S51})$$

Using these results, we obtain for Eq. (S40)

$$\begin{aligned} \mathcal{E}(\mathbf{Q}) \sum_{n \alpha \mathbf{k}} |z_{\mathbf{k} \alpha n}(\mathbf{Q})|^2 &= \sum_{n \mathbf{k} \alpha \beta} z_{\mathbf{k} \alpha n}^*(\mathbf{Q}) h(\mathbf{k} + \mathbf{Q})_{\alpha \beta} z_{\mathbf{k} \beta n}(\mathbf{Q}) - \sum_{n \alpha \mathbf{k}} |z_{\mathbf{k} \alpha n}(\mathbf{Q})|^2 E_n(\mathbf{k}) \\ &+ \frac{U}{N_c} \sum_{\alpha} \sum_{n \mathbf{k}} |z_{\mathbf{k} \alpha n}(\mathbf{Q})|^2 \sum_{l \mathbf{q}} \alpha \langle u_l(\mathbf{q}) | u_l(\mathbf{q}) \rangle_{\alpha} - \frac{U}{N_c} \sum_{n n' \alpha \mathbf{k} \mathbf{k}'} z_{\mathbf{k} \alpha n}^*(\mathbf{Q}) z_{\mathbf{k}' \alpha n'}(\mathbf{Q})_{\alpha} \langle u_{n'}(\mathbf{k}') | u_n(\mathbf{k}) \rangle_{\alpha}. \end{aligned} \quad (\text{S52})$$

Next, we take a partial derivative with respect to  $z_{\mathbf{k} \alpha n}^*(\mathbf{Q})$  and obtain

$$\begin{aligned} \mathcal{E}(\mathbf{Q}) z_{\mathbf{k} \alpha n}(\mathbf{Q}) &= \sum_{\beta} h(\mathbf{k} + \mathbf{Q})_{\alpha \beta} z_{\mathbf{k} \beta n}(\mathbf{Q}) - z_{\mathbf{k} \alpha n}(\mathbf{Q}) E_n(\mathbf{k}) + \frac{U}{N_c} z_{\mathbf{k} \alpha n}(\mathbf{Q}) \sum_{l \mathbf{q}} \alpha \langle u_l(\mathbf{q}) | u_l(\mathbf{q}) \rangle_{\alpha} \\ &- \frac{U}{N_c} \sum_{n' \mathbf{k}'} z_{\mathbf{k}' \alpha n'}(\mathbf{Q})_{\alpha} \langle u_{n'}(\mathbf{k}') | u_n(\mathbf{k}) \rangle_{\alpha}. \end{aligned} \quad (\text{S53})$$

This equation can be solved by converting it to an eigenvalue problem [45],

$$\mathcal{E}(\mathbf{Q}) z_{\mathbf{k} \alpha n}(\mathbf{Q}) = \sum_{\mathbf{k}' \beta n'} \mathcal{H}_{\mathbf{k} \alpha n, \mathbf{k}' \beta n'}^{SE}(\mathbf{Q}) z_{\mathbf{k}' \beta n'}(\mathbf{Q}), \quad (\text{S54})$$

where

$$\begin{aligned} \mathcal{H}_{\mathbf{k} \alpha n, \mathbf{k}' \beta n'}^{SE}(\mathbf{Q}) &= h(\mathbf{k} + \mathbf{Q})_{\alpha \beta} \delta_{\mathbf{k} \mathbf{k}'} \delta_{n n'} - E_n(\mathbf{k}) \delta_{\mathbf{k} \mathbf{k}'} \delta_{\alpha \beta} \delta_{n n'} + \frac{U}{N_c} \sum_{l \mathbf{q}} \alpha \langle u_l(\mathbf{q}) | u_l(\mathbf{q}) \rangle_{\alpha} \delta_{\mathbf{k} \mathbf{k}'} \delta_{\alpha \beta} \delta_{n n'} \\ &- \frac{U}{N_c} \alpha \langle u_{n'}(\mathbf{k}') | u_n(\mathbf{k}) \rangle_{\alpha} \delta_{\alpha \beta} \end{aligned} \quad (\text{S55})$$

is the spin excitation Hamiltonian whose rows and columns are indexed by  $\mathbf{k} \alpha n$  and  $\mathbf{k}' \beta n'$ , respectively.

Note that the only approximation we used is the definition of the spin excitation energy in Eq. (S40), which is inevitable due to the failure of Eq. (S39). Other than this, the spin excitation energy is exact, which we explicitly proved using Wick's theorem.

#### S4. SPIN EXCITATIONS AND THE GOLDSTONE MODE

In this Appendix, we introduce noteworthy aspects of the spin excitation spectrum. As illustrated in Fig. 1(c) of the main text, spin excitations consist of two parts. The first part is the quasiparticle excitations which form the Stoner continuum, whose energy scales linearly with  $U$ . The second part encompasses the  $N_{orb}$  collective excitations, also known as *spin waves*, which exist below the Stoner continuum. Contrary to the quasiparticle excitations, the spin wave energy reaches an upper bound determined by  $h(\mathbf{k})$  as  $U$  increases. The spin waves further consist of  $N_{orb} - 1$

gapped modes and 1 gapless mode, where the latter corresponds to a Goldstone boson generated by spontaneous symmetry breaking of the  $SU(2)$  group.

Let us solve for the gapless mode at  $\mathbf{Q} = \mathbf{0}$ . First, note that  $\mathcal{E}_G(\mathbf{0}) = 0$  indicates that the Goldstone mode at  $\mathbf{Q} = \mathbf{0}$  corresponds to another ground state of  $H$  with  $S_{tot}^z = S_{max} - 1$ . Since the ground states are given by  $S_{tot}^-|GS\rangle$ , we can intuitively predict that  $|\mathbf{Q}\rangle$  will be given by  $S_{tot}^-|\Phi\rangle$ . Let  $\psi_{n\mathbf{k}\sigma}^\dagger = \sum_{\alpha}^{N_{orb}} |u_n(\mathbf{k})\rangle_{\alpha} c_{\mathbf{k}\alpha\sigma}^\dagger$  denote the creation operator of the  $n$ -th band of the kinetic Hamiltonian. In terms of this operator, we obtain

$$S_{tot}^- = \sum_{i\alpha} c_{i\alpha\downarrow}^\dagger c_{i\alpha\uparrow} = \sum_{\mathbf{k}\alpha} c_{\mathbf{k}\alpha\downarrow}^\dagger c_{\mathbf{k}\alpha\uparrow} = \sum_{\mathbf{k}\alpha mn} \psi_{m\mathbf{k}\downarrow}^\dagger \psi_{n\mathbf{k}\uparrow} \cdot {}_{\alpha} \langle u_m(\mathbf{k}) | u_n(\mathbf{k}) \rangle_{\alpha} = \sum_{\mathbf{k}n} \psi_{n\mathbf{k}\downarrow}^\dagger \psi_{n\mathbf{k}\uparrow}, \quad (\text{S56})$$

where the sum over  $\alpha, m, n$  runs through  $1, \dots, N_{orb}$ . Combined with Eq. (S38), we obtain

$$z_{\mathbf{k}\alpha n}(\mathbf{0}) = |u_n(\mathbf{k})\rangle_{\alpha} \quad (\text{S57})$$

for the gapless mode. We verify that this does indeed correspond to the gapless mode by substituting into Eq. (S54) as follows.

$$\begin{aligned} \sum_{n'\mathbf{k}'\beta} \mathcal{H}_{\mathbf{k}\alpha n, \mathbf{k}'\beta n'}^{SE}(\mathbf{0}) |u_{n'}(\mathbf{k}')\rangle_{\beta} &= \sum_{n'\mathbf{k}'\beta} \left[ \{h(\mathbf{k})_{\alpha\beta} - E_n(\mathbf{k})\delta_{\alpha\beta}\} \delta_{\mathbf{k}\mathbf{k}'} \delta_{nn'} + \frac{U}{N_c} \left\{ \sum_{\mathbf{q}l} {}_{\alpha} \langle u_l(\mathbf{q}) | u_l(\mathbf{q}) \rangle_{\alpha} \delta_{\mathbf{k}\mathbf{k}'} \delta_{nn'} \right. \right. \\ &\quad \left. \left. - {}_{\alpha} \langle u_{n'}(\mathbf{k}') | u_n(\mathbf{k}) \rangle_{\alpha} \right\} \delta_{\alpha\beta} \right] |u_{n'}(\mathbf{k}')\rangle_{\beta} \\ &= \sum_{\beta} h(\mathbf{k})_{\alpha\beta} |u_n(\mathbf{k})\rangle_{\beta} - E_n(\mathbf{k}) |u_n(\mathbf{k})\rangle_{\alpha} + \frac{U}{N_c} \sum_{\mathbf{q}l} {}_{\alpha} \langle u_l(\mathbf{q}) | u_l(\mathbf{q}) \rangle_{\alpha} |u_n(\mathbf{k})\rangle_{\alpha} \\ &\quad - \frac{U}{N_c} \sum_{n'\mathbf{k}'} {}_{\alpha} \langle u_{n'}(\mathbf{k}') | u_n(\mathbf{k}) \rangle_{\alpha} |u_{n'}(\mathbf{k}')\rangle_{\alpha} \\ &= E_n(\mathbf{k}) |u_n(\mathbf{k})\rangle_{\alpha} - E_n(\mathbf{k}) |u_n(\mathbf{k})\rangle_{\alpha} \\ &\quad + \frac{U}{N_c} \left( \sum_{\mathbf{q}l} {}_{\alpha} \langle u_l(\mathbf{q}) | u_l(\mathbf{q}) \rangle_{\alpha} - \sum_{n'\mathbf{k}'} {}_{\alpha} \langle u_{n'}(\mathbf{k}') | u_{n'}(\mathbf{k}') \rangle_{\alpha} \right) |u_n(\mathbf{k})\rangle_{\alpha} \\ &= 0, \end{aligned} \quad (\text{S58})$$

where  $n', l$  are summed over  $1, \dots, N_{occ}$ . Thus, Eq. (S57) solves the Goldstone mode mode at  $\mathbf{Q} = \mathbf{0}$ .

Note that spin excitations with negative energy imply that we have assumed the wrong ground state when calculating  $\mathcal{H}^{SE}$ . Conversely, for a saturated ferromagnet, the gapless magnon mode is the nondegenerate ground state of  $\mathcal{H}^{SE}(\mathbf{0})$ , since the other spin excitations are gapped. Furthermore,  $\mathcal{E}_G(\mathbf{Q}) > 0$  is required, since any ground state of  $H$  must have maximal total spin, which is impossible for an arbitrary  $\mathbf{Q}$ . This implies that  $\mathbf{Q} = \mathbf{0}$  corresponds to the global minimum of  $\mathcal{E}_G(\mathbf{Q})$ . Expanding around  $\Gamma$ , we obtain

$$\mathcal{E}_G(\mathbf{Q}) = \mathcal{E}_G(\mathbf{0}) + Q_{\mu} \partial_{\mu} \mathcal{E}_G(\mathbf{Q})|_{\mathbf{Q}=\mathbf{0}} + \frac{Q_{\mu} Q_{\nu}}{2} \partial_{\mu} \partial_{\nu} \mathcal{E}_G(\mathbf{Q})|_{\mathbf{Q}=\mathbf{0}} + O(Q^3), \quad (\text{S59})$$

where the repeated indices are summed over. Thus, the linear term must vanish, and the spin stiffness  $D_{\mu\nu} \equiv \partial_{\mu} \partial_{\nu} \mathcal{E}_G(\mathbf{Q})|_{\mathbf{Q}=\mathbf{0}}$  must be a positive definite tensor. Using the Feynman-Hellmann theorem [80, 81], we show that the first condition is always satisfied:

$$\begin{aligned} \partial_{\mu} \mathcal{E}_G(\mathbf{Q})|_{\mathbf{Q}=\mathbf{0}} &= \frac{\sum_{\mathbf{k}\alpha n} \sum_{\mathbf{k}'\beta n'} \partial_{\mu} \mathcal{H}^{SE}(\mathbf{Q})|_{\mathbf{Q}=\mathbf{0}} z_{\mathbf{k}\alpha n}^*(\mathbf{0}) z_{\mathbf{k}'\beta n'}(\mathbf{0})}{\sum_{n\alpha\mathbf{k}} |z_{n\alpha\mathbf{k}}(\mathbf{0})|^2} \\ &= \frac{1}{N_{tot}} \sum_{n\mathbf{k}} \langle u_n(\mathbf{k}) | \frac{\partial h(\mathbf{k} + \mathbf{Q})}{\partial Q_{\mu}} \Big|_{\mathbf{Q}=\mathbf{0}} | u_n(\mathbf{k}) \rangle \\ &= \frac{1}{N_{tot}} \sum_{n\mathbf{k}} \langle u_n(\mathbf{k}) | \partial_{\mu} h(\mathbf{k}) | u_n(\mathbf{k}) \rangle \\ &= \frac{1}{N_{tot}} \sum_{n\mathbf{k}} \partial_{\mu} E_n(\mathbf{k}) \\ &= 0, \end{aligned} \quad (\text{S60})$$

where the first and fourth equality comes from the Feynman-Hellman theorem, and the last equality comes from the fact that  $E_n(\mathbf{k})$  is periodic throughout the 1st Brillouin zone (BZ). Therefore, a necessary but not sufficient condition for saturated ferromagnetism is that  $D_{\mu\nu}$  is a positive definite tensor.

### S5. APPROXIMATION TO THE GOLDSTONE MODE

In this Appendix, we derive the perturbative expansion of the Goldstone mode of the spin excitation spectrum, and discuss its properties. Let us describe the eigensystem of the spin excitation Hamiltonian as

$$\mathcal{H}^{SE}(\mathbf{Q})|z_n(\mathbf{Q})\rangle = \mathcal{E}_n(\mathbf{Q})|z_n(\mathbf{Q})\rangle \quad (n = 1, \dots, N_{tot}N_{orb}). \quad (\text{S61})$$

Due to the complexity of  $\mathcal{H}^{SE}(\mathbf{Q})$ , it is impossible to find an analytic solution. Thus, we obtain a perturbative expression by separating the terms as

$$\mathcal{H}^{SE}(\mathbf{Q}) = \mathcal{H}^{SE}(\mathbf{0}) + V(\mathbf{Q}), \quad (\text{S62})$$

where the unperturbed Hamiltonian is given by

$$\mathcal{H}_{\mathbf{k}\alpha n, \mathbf{k}'\beta n'}^{SE}(\mathbf{0}) = [h(\mathbf{k})_{\alpha\beta} - E_n(\mathbf{k})\delta_{\alpha\beta}]\delta_{\mathbf{k}\mathbf{k}'}\delta_{nn'} + \frac{U}{N_c} \left[ \sum_{\mathbf{q}} \sum_l^{N_c} \alpha \langle u_l(\mathbf{q}) | u_l(\mathbf{q}) \rangle_{\alpha} \delta_{\mathbf{k}\mathbf{k}'}\delta_{nn'} - \alpha \langle u_{n'}(\mathbf{k}') | u_n(\mathbf{k}) \rangle_{\alpha} \right] \delta_{\alpha\beta}, \quad (\text{S63})$$

and the perturbation is given by

$$V_{\mathbf{k}\alpha n, \mathbf{k}'\beta n'}(\mathbf{Q}) = [h(\mathbf{k} + \mathbf{Q}) - h(\mathbf{k})]_{\alpha\beta} \delta_{\mathbf{k}\mathbf{k}'}\delta_{nn'}. \quad (\text{S64})$$

Then, the Goldstone mode for a ferromagnetic state is given by

$$\begin{aligned} \mathcal{E}_G(\mathbf{Q}) &= \mathcal{E}_G^{(1)}(\mathbf{Q}) + \mathcal{E}_G^{(2)}(\mathbf{Q}) + \dots \\ &= \langle z_1(\mathbf{0}) | V(\mathbf{Q}) | z_1(\mathbf{0}) \rangle - \sum_{n>1} \frac{|\langle z_1(\mathbf{0}) | V(\mathbf{Q}) | z_n(\mathbf{0}) \rangle|^2}{\mathcal{E}_n(\mathbf{0})} + \dots \end{aligned} \quad (\text{S65})$$

Note that such perturbative expansion is only justified when the unperturbed Hamiltonian is much larger than the perturbation. Since the former contains  $U$ -linear terms, this analysis is valid in the  $U \rightarrow \infty$  limit. Even so, the first order term serves as a rigorous upper bound of  $\mathcal{E}_G(\mathbf{Q})$  for any  $U$ . To show this, note that

$$\mathcal{E}_G(\mathbf{Q}) = \langle z_1(\mathbf{Q}) | \mathcal{H}^{SE}(\mathbf{Q}) | z_1(\mathbf{Q}) \rangle \leq \langle v | \mathcal{H}^{SE}(\mathbf{Q}) | v \rangle \quad (\text{S66})$$

for an arbitrary vector  $|v\rangle$ , since  $|z_1(\mathbf{Q})\rangle$  is the true ground state eigenvector of  $\mathcal{H}^{SE}(\mathbf{Q})$ . Setting  $|v\rangle = |z_1(\mathbf{0})\rangle$ , we obtain the desired result.

#### A. First order perturbation theory

In the strongly correlated limit, we have verified in various models that first order perturbation is sufficient for determining the stability of the true Goldstone model  $\mathcal{E}_G(\mathbf{Q})$ ; in fact, in many cases,  $\mathcal{E}_G(\mathbf{Q})$  saturates to  $\mathcal{E}_G^{(1)}(\mathbf{Q})$  at small  $\mathbf{Q}$  when the *minimal metric condition* is satisfied. In more mathematical terms, resurgence does not occur from second order perturbation in this series. Thus, we focus on the first order term. Using  $|z_1(\mathbf{0})\rangle_{\mathbf{k}\alpha n} = \frac{|u_n(\mathbf{k})\rangle_{\alpha}}{\sqrt{N_{tot}}}$  for the (normalized) Goldstone mode, we obtain

$$\begin{aligned} \mathcal{E}_G^{(1)}(\mathbf{Q}) &= \langle z_1(\mathbf{0}) | V(\mathbf{Q}) | z_1(\mathbf{0}) \rangle \\ &= \frac{1}{N_{tot}} \sum_{\mathbf{k}} \sum_n^{N_{occ}} \langle u_n(\mathbf{k}) | h(\mathbf{k} + \mathbf{Q}) - h(\mathbf{k}) | u_n(\mathbf{k}) \rangle \\ &= \frac{1}{N_{tot}} \sum_{\mathbf{k}} \text{Tr}[(h(\mathbf{k} + \mathbf{Q}) - h(\mathbf{k}))P(\mathbf{k})]. \end{aligned} \quad (\text{S67})$$

We show that this term is always non-negative. To do this, let us assume that  $I_l \subset \{1, \dots, N_{orb}\}$  ( $l = 1, \dots, l_{tot}$ ) indexes  $|I_l|$  bands degenerate at every momentum, with energy  $\tilde{E}_l(\mathbf{k}) = E_{\sum_{l' < l} |I_{l'}| + 1}(\mathbf{k})$ . Moreover, we assume that  $N_{occ} = \sum_{l=1}^{l_{max}} |I_l|$ . For example, in a 3- band system with 2 occupied bands, which obeys  $E_1(\mathbf{k}) = E_2(\mathbf{k})$  at every  $\mathbf{k}$ ,



then  $I_1 = \{1, 2\}$  with  $\tilde{E}_1(\mathbf{k}) = E_1(\mathbf{k})$ , and  $I_2 = \{3\}$  with  $\tilde{E}_2(\mathbf{k}) = E_3(\mathbf{k})$ . In addition,  $l_{max} = 1$  and  $l_{tot} = 2$ . Then, the kinetic Hamiltonian is expressed as

$$h(\mathbf{k}) = \sum_l \tilde{E}_l(\mathbf{k}) \tilde{P}_l(\mathbf{k}) \quad (\tilde{P}_l(\mathbf{k}) = \sum_{n \in I_l} |u_n(\mathbf{k})\rangle \langle u_n(\mathbf{k})|). \quad (\text{S68})$$

We now claim that for any projector  $\mathcal{P}$  onto an  $N_{occ}$ -dimensional subspace,

$$Tr[h(\mathbf{k})\mathcal{P}] \geq \sum_n^{N_{occ}} E_n(\mathbf{k}), \quad (\text{S69})$$

and that the equality saturates iff  $\mathcal{P} = P(\mathbf{k})$ . The proof is as follows. Let

$$\alpha_l \equiv Tr[\tilde{P}_l(\mathbf{k})\mathcal{P}]. \quad (\text{S70})$$

Since  $\sum_l^{l_{tot}} \tilde{P}_l(\mathbf{k}) = \mathbb{1}$ , one has  $\sum_l^{l_{tot}} \alpha_l = N_{occ}$ . Moreover, one finds

$$0 \leq \alpha_l = \sum_{n \in I_l} \langle u_n(\mathbf{k}) | \mathcal{P} | u_n(\mathbf{k}) \rangle \leq |I_l|. \quad (\text{S71})$$

Then, the left hand side of Eq. (S69) simply reduces to

$$Tr[h(\mathbf{k})\mathcal{P}] = \sum_l^{l_{tot}} Tr[\tilde{E}_l(\mathbf{k}) \tilde{P}_l(\mathbf{k}) \mathcal{P}] = \sum_l^{l_{tot}} \alpha_l \tilde{E}_l(\mathbf{k}). \quad (\text{S72})$$

Clearly, this is minimized iff  $\alpha_l = |I_l|$  (0) for  $l \leq l_{max}$  ( $l > l_{max}$ ). From Eq. (S16), it readily follows that

$$\mathcal{P} = \mathcal{P} \sum_l^{l_{tot}} \tilde{P}_l(\mathbf{k}) = \mathcal{P} \sum_l^{l_{max}} \tilde{P}_l(\mathbf{k}) = \mathcal{P} P(\mathbf{k}). \quad (\text{S73})$$

This implies that the quantum distance between two projectors with equal trace,  $\mathcal{P}$  and  $P(\mathbf{k})$ , vanishes, which is equivalent to  $\mathcal{P} = P(\mathbf{k})$ .  $\square$

Applying this to  $\mathcal{E}_G^{(1)}(\mathbf{Q})$ , we obtain

$$\mathcal{E}_G^{(1)}(\mathbf{Q}) = \frac{1}{N_{tot}} \sum_{\mathbf{k}} Tr[(h(\mathbf{k} + \mathbf{Q}) - h(\mathbf{k}))P(\mathbf{k})] \geq \frac{1}{N_{tot}} \sum_{n\mathbf{k}} (E_n(\mathbf{k} + \mathbf{Q}) - E_n(\mathbf{k})) = 0, \quad (\text{S74})$$

where the lower bound saturates iff  $P(\mathbf{k} + \mathbf{Q}) = P(\mathbf{k})$  for every  $\mathbf{k}$ . In terms of quantum geometry, this means that  $s(\mathbf{k}, \mathbf{k} + \mathbf{Q})^2 = 0$  for every  $\mathbf{k}$ . As discussed in the main text, the stability condition at  $\mathbf{Q} = \mathbf{0}$  requires a positive definite quantum metric integral.

Expanding  $\mathcal{E}_G^{(1)}(\mathbf{Q})$  up to quadratic terms, we obtain

$$\begin{aligned} \mathcal{E}_G^{(1)}(\mathbf{Q}) &= \frac{1}{2} Q_\mu Q_\nu \partial_\mu \partial_\nu \mathcal{E}_G(\mathbf{Q})|_{\mathbf{Q}=\mathbf{0}} \\ &= \frac{Q_\mu Q_\nu}{2N_{tot}} \sum_{\mathbf{k}} \sum_n^{N_{occ}} \langle u_n(\mathbf{k}) | \frac{\partial^2 h(\mathbf{k} + \mathbf{Q})}{\partial Q_\mu \partial Q_\nu} \Big|_{\mathbf{Q}=\mathbf{0}} | u_n(\mathbf{k}) \rangle \\ &= \frac{Q_\mu Q_\nu}{2N_{tot}} \sum_{\mathbf{k}} \sum_n^{N_{occ}} \langle u_n(\mathbf{k}) | \partial_\mu \partial_\nu h(\mathbf{k}) | u_n(\mathbf{k}) \rangle. \end{aligned} \quad (\text{S75})$$

Inserting a resolution of identity, we obtain

$$\begin{aligned} \mathcal{E}_G^{(1)}(\mathbf{Q}) &= \frac{Q_\mu Q_\nu}{2N_{tot}} \sum_{\mathbf{k}} \sum_n^{N_{occ}} \sum_m^{N_{orb}} \langle u_n(\mathbf{k}) | \left[ \partial_\mu \partial_\nu | u_m(\mathbf{k}) \rangle \langle u_m(\mathbf{k}) | E_m(\mathbf{k}) \right] | u_n(\mathbf{k}) \rangle \\ &= \frac{Q_\mu Q_\nu}{2N_{tot}} \sum_{\mathbf{k}} \sum_n^{N_{occ}} \sum_m^{N_{orb}} \langle u_n(\mathbf{k}) | \end{aligned}$$

$$\begin{aligned}
& \left[ |\partial_\mu \partial_\nu u_m(\mathbf{k})\rangle \langle u_m(\mathbf{k})| E_m(\mathbf{k}) + |\partial_\mu u_m(\mathbf{k})\rangle \langle \partial_\nu u_m(\mathbf{k})| E_m(\mathbf{k}) + |\partial_\mu u_m(\mathbf{k})\rangle \langle u_m(\mathbf{k})| \partial_\nu E_m(\mathbf{k}) \right. \\
& + |\partial_\nu u_m(\mathbf{k})\rangle \langle \partial_\mu u_m(\mathbf{k})| E_m(\mathbf{k}) + |u_m(\mathbf{k})\rangle \langle \partial_\mu \partial_\nu u_m(\mathbf{k})| E_m(\mathbf{k}) + |u_m(\mathbf{k})\rangle \langle \partial_\mu u_m(\mathbf{k})| \partial_\nu E_m(\mathbf{k}) \\
& \left. + |\partial_\nu u_m(\mathbf{k})\rangle \langle u_m(\mathbf{k})| \partial_\mu E_m(\mathbf{k}) + |u_m(\mathbf{k})\rangle \langle \partial_\nu u_m(\mathbf{k})| \partial_\mu E_m(\mathbf{k}) + |u_m(\mathbf{k})\rangle \langle u_m(\mathbf{k})| \partial_\mu \partial_\nu E_m(\mathbf{k}) \right] |u_n(\mathbf{k})\rangle \\
& = \frac{Q_\mu Q_\nu}{2N_{tot}} \sum_{\mathbf{k}} \sum_n^{N_c} \left\{ \langle u_n(\mathbf{k})| \partial_\mu \partial_\nu u_n(\mathbf{k}) \rangle E_n(\mathbf{k}) + \langle u_n(\mathbf{k})| \partial_\mu u_n(\mathbf{k}) \rangle \partial_\nu E_n(\mathbf{k}) + \langle \partial_\mu \partial_\nu u_n(\mathbf{k})| u_n(\mathbf{k}) \rangle E_n(\mathbf{k}) \right. \\
& + \langle \partial_\mu u_n(\mathbf{k})| u_n(\mathbf{k}) \rangle \partial_\nu E_n(\mathbf{k}) + \langle u_n(\mathbf{k})| \partial_\nu u_n(\mathbf{k}) \rangle \partial_\mu E_n(\mathbf{k}) + \langle \partial_\nu u_n(\mathbf{k})| u_n(\mathbf{k}) \rangle \partial_\mu E_n(\mathbf{k}) + \partial_\mu \partial_\nu E_n(\mathbf{k}) \\
& \left. + \sum_m^{N_{orb}} \left( \langle u_n(\mathbf{k})| \partial_\mu u_m(\mathbf{k}) \rangle \langle \partial_\nu u_m(\mathbf{k})| u_n(\mathbf{k}) \rangle + \langle u_n(\mathbf{k})| \partial_\nu u_m(\mathbf{k}) \rangle \langle \partial_\mu u_m(\mathbf{k})| u_n(\mathbf{k}) \rangle \right) E_m(\mathbf{k}) \right\}. \quad (S76)
\end{aligned}$$

To simplify Eq. (S76), we use the following identities:

$$\begin{aligned}
& \langle u_m(\mathbf{k})| u_n(\mathbf{k}) \rangle = \delta_{m\nu}, \quad \langle \partial_\mu u_m(\mathbf{k})| u_n(\mathbf{k}) \rangle + \langle u_m(\mathbf{k})| \partial_\mu u_n(\mathbf{k}) \rangle = 0, \quad \text{and} \\
& \langle \partial_\mu \partial_\nu u_m(\mathbf{k})| u_n(\mathbf{k}) \rangle + \langle u_m(\mathbf{k})| \partial_\mu \partial_\nu u_n(\mathbf{k}) \rangle + \langle \partial_\mu u_m(\mathbf{k})| \partial_\nu u_n(\mathbf{k}) \rangle + \langle \partial_\nu u_m(\mathbf{k})| \partial_\mu u_n(\mathbf{k}) \rangle = 0. \quad (S77)
\end{aligned}$$

Then, we obtain

$$\begin{aligned}
\mathcal{E}_G^{(1)}(\mathbf{Q}) &= \frac{Q_\mu Q_\nu}{2N_{tot}} \sum_{\mathbf{k}} \sum_n^{N_c} \left[ \partial_\mu \partial_\nu E_n(\mathbf{k}) - (\langle \partial_\mu u_n(\mathbf{k})| \partial_\nu u_n(\mathbf{k}) \rangle + \langle \partial_\nu u_n(\mathbf{k})| \partial_\mu u_n(\mathbf{k}) \rangle) E_n(\mathbf{k}) \right. \\
& + \sum_m^{N_{orb}} \left( \langle \partial_\mu u_m(\mathbf{k})| u_n(\mathbf{k}) \rangle \langle u_n(\mathbf{k})| \partial_\nu u_m(\mathbf{k}) \rangle + \langle \partial_\nu u_m(\mathbf{k})| u_n(\mathbf{k}) \rangle \langle u_n(\mathbf{k})| \partial_\mu u_m(\mathbf{k}) \rangle \right) E_m(\mathbf{k}) \Big] \\
&= \frac{Q_\mu Q_\nu}{2N_{tot}} \sum_{\mathbf{k}} \sum_n^{N_c} \left[ \partial_\mu \partial_\nu E_n(\mathbf{k}) + \sum_m^{N_{orb}} \left( \langle \partial_\mu u_m(\mathbf{k})| u_n(\mathbf{k}) \rangle \langle u_n(\mathbf{k})| \partial_\nu u_m(\mathbf{k}) \rangle + \mu \leftrightarrow \nu \right) E_m(\mathbf{k}) \right. \\
& - \sum_m^{N_{orb}} \left( \langle \partial_\mu u_n(\mathbf{k})| u_m(\mathbf{k}) \rangle \langle u_m(\mathbf{k})| \partial_\nu u_n(\mathbf{k}) \rangle + \langle \partial_\nu u_n(\mathbf{k})| u_m(\mathbf{k}) \rangle \langle u_m(\mathbf{k})| \partial_\mu u_n(\mathbf{k}) \rangle \right) E_n(\mathbf{k}) \Big] \\
&= \frac{Q_\mu Q_\nu}{2N_{tot}} \sum_{\mathbf{k}} \sum_n^{N_c} \left[ \partial_\mu \partial_\nu E_n(\mathbf{k}) + \sum_m^{N_{orb}} \left( \langle \partial_\mu u_m(\mathbf{k})| u_n(\mathbf{k}) \rangle \langle u_n(\mathbf{k})| \partial_\nu u_m(\mathbf{k}) \rangle + \mu \leftrightarrow \nu \right) E_m(\mathbf{k}) \right. \\
& - \sum_m^{N_{orb}} \left( \langle u_n(\mathbf{k})| \partial_\mu u_m(\mathbf{k}) \rangle \langle \partial_\nu u_m(\mathbf{k})| u_n(\mathbf{k}) \rangle + \langle u_n(\mathbf{k})| \partial_\nu u_m(\mathbf{k}) \rangle \langle \partial_\mu u_m(\mathbf{k})| u_n(\mathbf{k}) \rangle \right) E_n(\mathbf{k}) \Big] \\
&= \frac{Q_\mu Q_\nu}{2N_{tot}} \sum_{\mathbf{k}} \left[ \sum_n^{N_{occ}} \partial_\mu \partial_\nu E_n(\mathbf{k}) + \sum_m^{N_{orb}} \sum_n^{N_{occ}} (E_m(\mathbf{k}) - E_n(\mathbf{k})) (\langle \partial_\mu u_m(\mathbf{k})| u_n(\mathbf{k}) \rangle \langle u_n(\mathbf{k})| \partial_\nu u_m(\mathbf{k}) \rangle + \mu \leftrightarrow \nu) \right], \quad (S78)
\end{aligned}$$

where we have inserted a resolution of identity to obtain the second equality. In terms of  $\chi_{\mu\nu}^{mn}(\mathbf{k})$ , this reduces to

$$\begin{aligned}
\mathcal{E}_G^{(1)}(\mathbf{Q}) &= \frac{Q_\mu Q_\nu}{2N_{tot}} \sum_{\mathbf{k}} \left[ \sum_n^{N_{occ}} \partial_\mu \partial_\nu E_n(\mathbf{k}) + \sum_m^{N_{orb}} \sum_n^{N_{occ}} (E_m(\mathbf{k}) - E_n(\mathbf{k})) (\chi_{\mu\nu}^{mn}(\mathbf{k}) + \chi_{\nu\mu}^{mn}(\mathbf{k})) \right] \\
&= \frac{Q_\mu Q_\nu}{2N_{tot}} \sum_{\mathbf{k}} \left[ \sum_n^{N_{occ}} \partial_\mu \partial_\nu E_n(\mathbf{k}) + 2 \sum_m^{N_{orb}} \sum_n^{N_{occ}} (E_m(\mathbf{k}) - E_n(\mathbf{k})) \chi_{\mu\nu}^{mn}(\mathbf{k}) \right], \quad (S79)
\end{aligned}$$

where we have interchanged the summation indices  $\mu$  and  $\nu$  of the last term to obtain the second equality. We further note that  $\chi_{\mu\nu}^{mn}(\mathbf{k}) = \chi_{\nu\mu}^{nm}(\mathbf{k})$ . Then, the terms with  $m \in \{1, \dots, N_{occ}\}$  in the second summation become 0 from the following relation:

$$\sum_{\mu\nu}^d \sum_m^{N_{occ}} \sum_n^{N_{occ}} (E_m(\mathbf{k}) - E_n(\mathbf{k})) \chi_{\mu\nu}^{mn}(\mathbf{k}) Q_\mu Q_\nu$$

$$\begin{aligned}
&= \sum_{\mu\nu}^d \sum_m^{N_{occ}} \sum_n^{N_{occ}} (E_n(\mathbf{k}) - E_m(\mathbf{k})) \chi_{\nu\mu}^{nm}(\mathbf{k}) Q_\mu Q_\nu \\
&= - \sum_{\mu\nu}^d \sum_m^{N_{occ}} \sum_n^{N_{occ}} (E_m(\mathbf{k}) - E_n(\mathbf{k})) \chi_{\mu\nu}^{mn}(\mathbf{k}) Q_\mu Q_\nu.
\end{aligned} \tag{S80}$$

Thus, we finally arrive at

$$\mathcal{E}_G^{(1)}(\mathbf{Q}) = \frac{Q_\mu Q_\nu}{2N_{tot}} \sum_{\mathbf{k}}^{N_c} \left[ \sum_n^{N_{occ}} \partial_\mu \partial_\nu E_n(\mathbf{k}) + 2 \sum_{m>N_{occ}}^{N_{orb}} \sum_n^{N_{occ}} (E_m(\mathbf{k}) - E_n(\mathbf{k})) \chi_{\mu\nu}^{mn}(\mathbf{k}) \right]. \tag{S81}$$

Note that the first term of this expression vanishes when  $E_n(\mathbf{k})$  are smooth and periodic. This is because integrating the derivative of a smooth periodic function over a period vanishes. In such cases, it is clear that the fidelity tensor determines whether the spin stiffness can be positive definite. On the other hand, when the occupied bands form a kink structure due to a band crossing with the unoccupied bands, the first term does not vanish. This may lead one to think that the singularity of the band structure, regardless of quantum geometry, can stabilize ferromagnetism. This is not the case, however, since a singularity in  $E_n(\mathbf{k})$  necessarily causes a divergence in  $\chi_{\mu\nu}^{mn}(\mathbf{k})$ . We prove this by contradiction. Without loss of generality, we set  $l_{max} = 1$  (see Eq. (S68)), and consider a band crossing at  $\mathbf{k}^*$ . Around this point, we assume that  $\partial_\mu \tilde{E}_1(\mathbf{k})$  is discontinuous, while  $\tilde{P}_1(\mathbf{k})$  is smooth. Let us now consider

$$h(\mathbf{k}) \tilde{P}_1(\mathbf{k}) = \tilde{E}_1(\mathbf{k}) \tilde{P}_1(\mathbf{k}). \tag{S82}$$

Since  $h(\mathbf{k})$  is smooth, this expression must be smooth; moreover,

$$\partial_\mu (h(\mathbf{k}) \tilde{P}_1(\mathbf{k})) = \partial_\mu \tilde{E}_1(\mathbf{k}) \tilde{P}_1(\mathbf{k}) + \tilde{E}_1(\mathbf{k}) \partial_\mu \tilde{P}_1(\mathbf{k}) \tag{S83}$$

must also be smooth. However,  $\partial_\mu \tilde{E}_1(\mathbf{k}) \tilde{P}_1(\mathbf{k})$  is discontinuous. Thus, a kink in the band structure necessarily induces a singularity in the occupied band eigenstates. Therefore,  $\mathcal{E}_G^{(1)}(\mathbf{Q}) > 0$  cannot occur without a nontrivial quantum geometry, even if the first term is finite.

### 1. Upper bound of the spin stiffness

In this Appendix, we prove that

$$\mathcal{E}_G(\mathbf{Q})|_{U<\infty} \leq \mathcal{E}_G(\mathbf{Q})|_{U\rightarrow\infty} \leq \mathcal{E}_G^{(1)}(\mathbf{Q}) \tag{S84}$$

implies

$$D_{\mu\mu}(U < \infty) \leq D_{\mu\mu}(U \rightarrow \infty) \leq D_{\mu\mu}^{(1)}. \tag{S85}$$

The proof follows directly in the following way. Consider two smooth analytic functions  $f$  and  $g$ , where  $f(\mathbf{0}) = g(\mathbf{0}) = 0$  and  $f(\mathbf{Q}) \leq g(\mathbf{Q})$ . Let  $F(\mathbf{Q}) = g(\mathbf{Q}) - f(\mathbf{Q}) \geq 0$ , with  $F(\mathbf{0}) = 0$ . This implies that Hessian of  $F(\mathbf{Q})$  defined by  $\mathfrak{D}_{\mu\nu} \equiv \frac{\partial^2 F(\mathbf{Q})}{\partial Q_\mu \partial Q_\nu} \big|_{\mathbf{Q}=\mathbf{0}}$  is positive semidefinite. This implies that the diagonal entries are greater than or equal to 0. Applying this to Eq. (S84) finishes the proof.

### B. Second order perturbation theory

In this Appendix, we discuss the condition where  $\lim_{U\rightarrow\infty} D_{\mu\nu} = D_{\mu\nu}^{(1)}$ . Starting from

$$\begin{aligned}
\mathcal{E}_G(\mathbf{Q}) &= \mathcal{E}_G^{(1)}(\mathbf{Q}) + \mathcal{E}_G^{(2)}(\mathbf{Q}) + \dots \\
&= \langle z_1(\mathbf{0}) | V(\mathbf{Q}) | z_1(\mathbf{0}) \rangle - \sum_{n>1} \frac{|\langle z_1(\mathbf{0}) | V(\mathbf{Q}) | z_n(\mathbf{0}) \rangle|^2}{\mathcal{E}_n(\mathbf{0})} + \dots,
\end{aligned} \tag{S86}$$

we find that

$$D_{\mu\nu} = D_{\mu\nu}^{(1)} + D_{\mu\nu}^{(2)}, \tag{S87}$$

where the higher order terms vanish due since they contain terms  $\langle z_n(\mathbf{0})|V(\mathbf{0})|z_1(\mathbf{0})\rangle = 0$ . Thus, we obtain

$$\lim_{U \rightarrow \infty} D_{\mu\nu} = D_{\mu\nu}^{(1)} \Leftrightarrow \lim_{U \rightarrow \infty} D_{\mu\nu}^{(2)} = 0, \quad (\text{S88})$$

since  $D_{\mu\nu}^{(1)}$  is independent of  $U$ . To find this condition, note that

$$\lim_{U \rightarrow \infty} \mathcal{E}_n(\mathbf{0}) \begin{cases} < \infty & (n \leq N_{orb}) \\ = \infty & (n > N_{orb}) \end{cases}, \quad (\text{S89})$$

that is, the energy of Stoner continuum states diverge, while the magnon modes saturate to a finite energy. This indicates that at  $U \rightarrow \infty$ , the  $N_{orb}$  magnon modes form a basis of the null space of the  $U$ -dependent part of  $\mathcal{H}^{SE}(\mathbf{0})$ . Note that this statement is only true in the strongly correlated limit, since  $|z_n(\mathbf{0})\rangle$  ( $n = 2, \dots, N_{orb}$ ) are a function of  $U$  in general. Thus, an equivalent condition for  $D_{\mu\nu}^{(2)} = 0$  may be obtained by expanding the second order perturbation up to quadratic order as

$$\begin{aligned} \lim_{U \rightarrow \infty} \mathcal{E}_G^{(2)}(\mathbf{Q}) &= -\frac{1}{2} Q_\mu Q_\nu \partial_\mu \partial_\nu \lim_{U \rightarrow \infty} \sum_{n=2}^{N_{orb}} \frac{|\langle z_1(\mathbf{0})|V(\mathbf{Q})|z_n(\mathbf{0})\rangle|^2}{\mathcal{E}_n(\mathbf{0})} \Big|_{\mathbf{Q}=\mathbf{0}} \\ &= -\frac{1}{2} Q_\mu Q_\nu \lim_{U \rightarrow \infty} \sum_{n=2}^{N_{orb}} \frac{\langle z_1(\mathbf{0})|\partial_\mu V(\mathbf{0})|z_n(\mathbf{0})\rangle \langle z_n(\mathbf{0})|\partial_\nu V(\mathbf{0})|z_1(\mathbf{0})\rangle + (\mu \leftrightarrow \nu)}{\mathcal{E}_n(\mathbf{0})} \\ &= -Q_\mu Q_\nu \lim_{U \rightarrow \infty} \sum_{n=2}^{N_{orb}} \frac{\langle z_1(\mathbf{0})|\partial_\mu V(\mathbf{0})|z_n(\mathbf{0})\rangle \langle z_n(\mathbf{0})|\partial_\nu V(\mathbf{0})|z_1(\mathbf{0})\rangle}{\mathcal{E}_n(\mathbf{0})} \\ &= 0, \end{aligned} \quad (\text{S90})$$

where the higher-order terms have been omitted. Defining  $|v\rangle = Q_\mu \partial_\mu V(\mathbf{0})|z_1(\mathbf{0})\rangle$ , the desired condition reduces to

$$\lim_{U \rightarrow \infty} \mathcal{E}_G^{(2)}(\mathbf{Q}) = - \lim_{U \rightarrow \infty} \sum_{n=2}^{N_{orb}} \frac{\langle v|z_n(\mathbf{0})\rangle \langle z_n(\mathbf{0})|v\rangle}{\mathcal{E}_n(\mathbf{0})} = 0. \quad (\text{S91})$$

Note that  $|z_n(\mathbf{0})\rangle \langle z_n(\mathbf{0})|$  is a positive semidefinite matrix. Thus, Eq. (S15) implies that Eq. (S91) is equivalent to  $\lim_{U \rightarrow \infty} |z_n(\mathbf{0})\rangle \langle z_n(\mathbf{0})|v\rangle = 0$  for any  $\mathbf{Q}$  and  $1 < n \leq N_{orb}$ . Since this condition also holds for  $n = 1$ , we find that

$$\lim_{U \rightarrow \infty} D_{\mu\nu}^{(2)} = 0 \quad \Leftrightarrow \quad P^0 \partial_\mu V(\mathbf{0})|z_1(\mathbf{0})\rangle = 0 \quad (\forall \mu), \quad (\text{S92})$$

where  $P^0$  is the projector onto the null space of the  $U$ -dependent part of  $\mathcal{H}^{SE}(\mathbf{0})$ .

Unfortunately, we are not aware of a simple solution to this problem, and believe that it requires exactly solving the  $N_{orb} - 1$  gapped magnon modes at  $\mathbf{Q} = \mathbf{0}$  for  $U \rightarrow \infty$ . However, model calculations suggest that the spin stiffness saturates to  $D_{\mu\nu}^{(1)}$  if the *minimal metric condition* is satisfied [28, 53, 82]. To understand this concept, note that the spin excitation spectrum calculated from Eq. (S55) is invariant upon transformations which preserve the hopping amplitudes while shifting the orbital positions. Physically, this is because the many-body spectrum of  $H$  is invariant under such transformations. However, this transformation affects the quantum metric and the maximally localized Wannier functions, which in turn impacts  $\mathcal{E}_G^{(1)}(\mathbf{Q})$ . Thus, one cannot directly equate the quantum metric to physical quantities independent of orbital positions. Instead, one must use the precise orbital positions which minimizes the quantum metric. Note that the minimal condition is satisfied if the orbitals originate from maximal Wyckoff positions including rotation (2D) or inversion symmetries. This is precisely the case in the kagomé lattice model and the flat band model in the main text, where the orbitals are placed on 3-fold rotation symmetric points.

As a demonstration, let us consider the wallpaper group  $p4$ , and place  $s$  orbitals on the  $2c$  maximal Wyckoff position as in Fig. S1(a). The onsite two-fold rotation symmetries enforce the minimal metric condition. Up to next-nearest neighbor hoppings, the single-particle Hamiltonian is given by

$$h(\mathbf{k}) = 2 \begin{pmatrix} t_1 \cos 2\pi k_1 + t_2 \cos 2\pi k_2 & (t_3 - it_4) \cos \pi(k_1 - k_2) + (t_3 + it_4) \cos \pi(k_1 + k_2) \\ (t_3 + it_4) \cos \pi(k_1 - k_2) + (t_3 - it_4) \cos \pi(k_1 + k_2) & t_1 \cos 2\pi k_2 + t_2 \cos 2\pi k_1 \end{pmatrix}, \quad (\text{S93})$$

which is the most general form containing up to next-nearest neighbor (NNN) hopping amplitudes. We plot the electron dispersion of  $h(\mathbf{k})$  in Fig. S2(b). The Goldstone mode dispersion in Fig. S1(c) shows the saturation of the upper bound at  $U \rightarrow \infty$ .



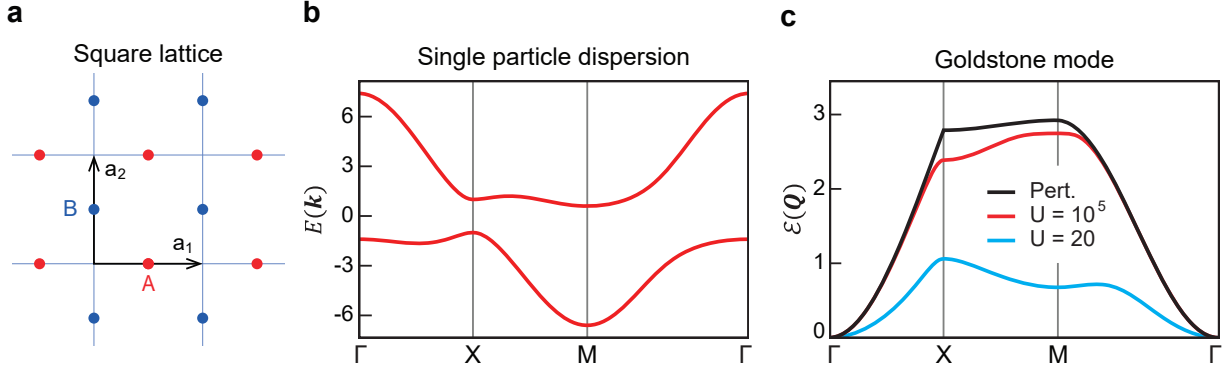


FIG. S1. **Spin excitations in the square lattice model.** (a) The square lattice in wallpaper group  $p4$ .  $s$  orbitals are placed on the  $2c$  maximal Wyckoff positions, which guarantees the minimal metric condition. (b) Single-particle electron dispersion of the square lattice model (Eq. (S93)) with  $t_1 = -1.2 - 0.7i$ ,  $t_2 = -0.5 + 2.6i$ ,  $v_1 = -1.7 - 0.4i$ ,  $v_2 = -1.6 + 0.9i$ . (c) Goldstone mode of the magnon spectrum for  $N_{occ} = 1$  occupied band at different interaction strengths. At large  $U$  (red), the Goldstone mode saturates to the first order perturbation (black) around  $\mathbf{Q} = 0$ .

As another example, consider the Haldane model [83] in Fig. S2(a), which obeys the minimal metric condition due to the onsite three-fold symmetry. The single-particle Hamiltonian is characterized by

$$h(\mathbf{k}) = t_1 \begin{pmatrix} 0 & f(\mathbf{k}) \\ f^*(\mathbf{k}) & 0 \end{pmatrix} + 2t_2(-\sin 2\pi k_1 + \sin 2\pi k_2 + \sin 2\pi(k_1 - k_2))\sigma_z, \quad (\text{S94})$$

where  $f(\mathbf{k}) = e^{-\frac{2\pi i}{3}(2k_1 - k_2)} + e^{\frac{2\pi i}{3}(k_1 + k_2)} + e^{\frac{2\pi i}{3}(k_1 - 2k_2)}$ , where  $t_1$  is the nearest-neighbor (NN) hopping amplitudes and  $t_2$  represents the NNN hopping which breaks the time reversal symmetry. In Fig. S2(b), we show the single particle band structure for  $t_1 = 1$  and  $t_2 = 0.5$ . In the inset, we plot the Wilson loop eigenvalue  $\theta(k_1)$  obtained by the path-ordered integral of the Berry connection along the  $\mathbf{b}_2$  direction (see Eq. (S1)), which shows that the occupied band has Chern number  $-1$  [84]. Due to the Wannier obstruction imposed by the nontrivial topology, this system has a large quantum metric integral, which stabilizes the Goldstone mode of the spin excitation in the strongly correlated limit (Fig. S2(c)). A comparison between the  $\mathcal{E}_G^{(1)}(\mathbf{Q})$  (black) and the true Goldstone mode energy at  $U = 10^5$  (red) clearly shows the validity of the approximation scheme in the strongly correlated limit.

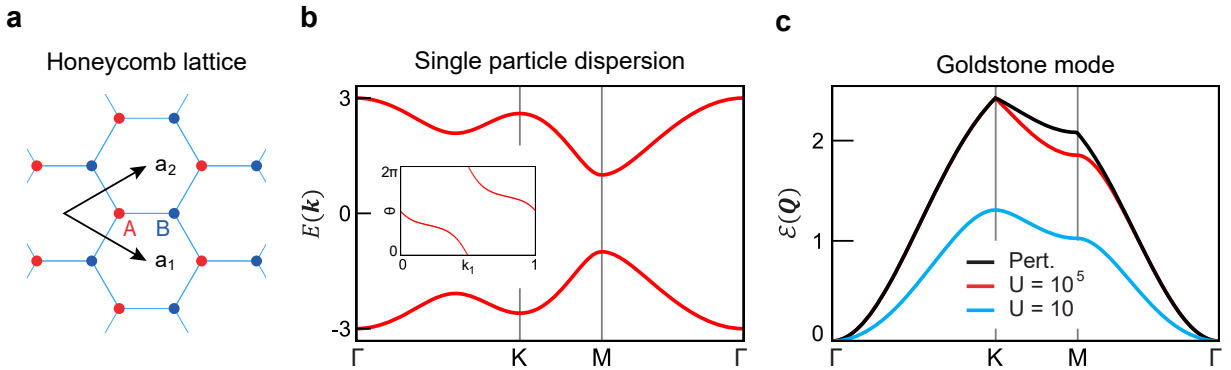


FIG. S2. **Spin excitations in the Haldane model.** (a) The honeycomb lattice. The  $A$  and  $B$  sites are placed on three-fold rotation invariant points, which enforces the minimal metric condition. (b) Single-particle electron dispersion of the Haldane model (Eq. (S94)) with  $t_1 = 1$ ,  $t_2 = 0.5$ . The inset is the Wilson loop eigenvalue plotted along the  $k_1$  direction (see Eq. (S1)), which shows that the occupied band has Chern number  $-1$ . (c) Goldstone mode of the magnon spectrum for  $N_{occ} = 1$  occupied band. At large  $U$  (red), the Goldstone mode saturates to the first order perturbation (black) around  $\mathbf{Q} = 0$ .

## S6. NUMERICAL CALCULATIONS ON THE NO-GO THEOREM

In this Appendix, we demonstrate the validity of the no-go theorem by calculating the magnon dispersion of half-filled models. Fig. S3(a) describes the magnon spectrum of the NN kagomé lattice at half filling. The magnon bands with negative energy indicate the instability of saturated ferromagnetism. Fig. S3(b) illustrates a representative example of a half-filled system with a single orbital, which is obtained from a 2D square lattice. To show the generality of the no-go theorem, we introduce arbitrary complex hopping amplitudes up to NNN, and break every symmetry other than SU(2) symmetry. The noninteracting Hamiltonian is given by

$$h(\mathbf{k}) = t_1 e^{ik_x} + t_2 e^{ik_y} + v_1 e^{i(k_x - k_y)} + v_2 e^{i(k_x + k_y)} + c.c., \quad (\text{S95})$$

where  $t_i$  and  $v_i$  denote the NN and NNN hopping amplitudes, respectively. The magnon spectrum with negative energy shown in Fig. S3(b) clearly indicates that saturated ferromagnetism is prohibited.

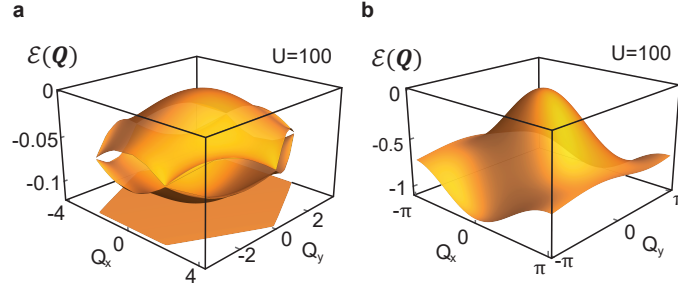


FIG. S3. **Negative spin-wave energy of half-filled Hubbard models.** (a) The kagomé lattice with  $t = 1$  and  $U = 100$ . (b) The square lattice model introduced in Eq. (S95) with  $t_1 = -1.2 - 0.7i$ ,  $t_2 = -0.5 + 2.6i$ ,  $v_1 = -1.7 - 0.4i$ ,  $v_2 = -1.6 + 0.9i$ , and  $U = 100$ .

## S7. MEAN-FIELD HAMILTONIAN OF SATURATED FERROMAGNETS

In this Appendix, we briefly mention the mean-field Hamiltonian used for calculating the spin-resolved electron band dispersion in Fig. 1(b). Following the main text, we assume that every occupied state has spin  $\uparrow$ . The mean-field Hamiltonian obtained by decoupling the many-body terms of the second line of Eq. (S3) is given by

$$H_{mf} = \sum_{\mathbf{k}\alpha\beta\sigma} h(\mathbf{k})_{\alpha\beta} c_{\mathbf{k}\alpha\sigma}^\dagger c_{\mathbf{k}\beta\sigma} + U \sum_{\mathbf{k}\alpha\sigma} \langle n_{\alpha-\sigma} \rangle c_{\mathbf{k}\alpha\sigma}^\dagger c_{\mathbf{k}\alpha\sigma} - U N_c \sum_{\alpha} \langle n_{\alpha\uparrow} \rangle \langle n_{\alpha\downarrow} \rangle, \quad (\text{S96})$$

where  $\langle n_{\alpha\sigma} \rangle = \langle c_{i\alpha\sigma}^\dagger c_{i\alpha\sigma} \rangle$  is the unit cell-independent orbital filling to be self-consistently determined. In the  $(\uparrow, \downarrow)^T \otimes (\alpha_1, \dots, \alpha_{N_{orb}})^T$  basis,  $H_{mf}(\mathbf{k})$  is a  $(2N_{orb} \times 2N_{orb})$  Hermitian matrix given by

$$H_{mf}(\mathbf{k}) = \begin{pmatrix} h_{\uparrow\uparrow}(\mathbf{k}) & h_{\uparrow\downarrow}(\mathbf{k}) \\ h_{\downarrow\uparrow}(\mathbf{k}) & h_{\downarrow\downarrow}(\mathbf{k}) \end{pmatrix} = \begin{pmatrix} h(\mathbf{k}) & 0 \\ 0 & h(\mathbf{k}) \end{pmatrix} + U \begin{pmatrix} \text{diag}(\mathbf{n}_\downarrow) & 0 \\ 0 & \text{diag}(\mathbf{n}_\uparrow) \end{pmatrix}, \quad (\text{S97})$$

where  $\mathbf{n}_\sigma = (\langle n_{1\sigma} \rangle, \dots, \langle n_{N_{orb}\sigma} \rangle)$ . Since the  $\downarrow$  bands are empty ( $\mathbf{n}_\downarrow = \mathbf{0}$ ), the Hamiltonian of occupied states (which have  $\uparrow$ ) is identical to  $h(\mathbf{k})$ . This observation underscores that the ground state of a saturated ferromagnet is fully determined by the noninteracting Hamiltonian. As an example, we present the mean-field band structure of a kagomé ferromagnet in Fig. 1(b) of the main text.